# Response to comments of Reviewers

We would like to thank all the Reviewers for their thoughtful and valuable comments, which helped us to improve the content and quality of our manuscript. We addressed all comments and included changes in the manuscript as follows:

Blue: Comments of Reviewer

Black: Answers of Authors

*Black, italic, quotation marks: "Changes in the manuscript"*

Page and line references in our answers refer to the reviewed manuscript.

Additional references and updated Figures with captions were inserted at the end of this revision after addressing the comments of the three Reviewers.

## Reviewer #1

Specific Comments:

**a) p. 1 line 11:** Define high spatial and temporal resolution. What is the resolution exactly?

**Answer:** We included a definition for high spatial and temporal resolution and changed the text to:

*"Vertical profiles of atmospheric variables in the SL at high spatial (meters) and temporal (1 Hz and better) resolution increase our understanding of these interactions, but are still challenging to measure appropriately."*

**b) p. 1 line 13:** Scanning lidar observations (of various kinds: Doppler, DIAL, Raman) can measure winds, temperature, moisture, and some trace gas quantities (such as ozone) with high-vertical and spatial resolution (on the order of meters to 10s of meters) at low elevations angles and over large horizontal areas close to the ground. Thus, the broad statement that 'remote sensing techniques ... are challenged to achieve sufficient detail near the ground' should be modified.

**Answer:** We agree with this and changed the sentence to:

"*At the same time, most remote sensing techniques and aircraft measurements have limitations to achieve sufficient detail close to the ground (up to about 50 m)."*

**c) p. 1 line 14:** Change 'horizontal sounding' to 'horizontal transect'. A 'sounding' implies a vertical profile by definition.

**Answer:** We changed the text to:

*"Vertical and horizontal transects of the PBL can be complemented by unmanned aerial*

*vehicles (UAV).”*

**d) p. 1 line 24:** Clarify that the UAV measures a continuous profile, in comparison that towers only measure at discrete levels where instrumentation are installed.

**Answer:** Since in this context it was pointed out that the vertical height of tower measurements was extended by UAV measurements, we think that at this point an explanation is not necessary. In addition, this is too much information for the abstract. Instead, we stated on p. 2, l. 3:

*“The operation of towers is fixed to a certain location and the vertical information is limited to the height of the tower as well as to discrete levels at the tower.”*

**e) p. 2 line 9:** Again, there have been studies using scanning lidar to make profiles where the minimum height above ground is 10-20 m (see Langford et al., 2015 (ozone profiles), Banta et al., 2013 (wind profiles), Yabuki et al. (water vapor), and Hammann et al., 2015 (temperature)). Data shown in these studies contradicts the statement that ground-based remote sensing cannot measure near the surface.

**Answer:** Looking at the literature you provided, it is indeed possible to measure at low altitudes with a LIDAR. But considering for example acoustic instruments, this is not the case. Therefore, we differentiated LIDAR and acoustic methods and changed the sentence. References were included, too:

*“Considering ground-based remote sensing methods, data of vertical profiles from low altitudes up to about 50 m above ground level (a.g.l.) are hardly usable (e.g. acoustic instruments), but possible with LIDARs applying certain scan patterns with low elevation angles at the position of such an instrument (Emeis, et al., 2009; Banta et al., 2013; Korhonen et al., 2014; Hammann et al., 2015).*

**f) p. 2 lines 10-14:** This paragraph seems out of place here. I recommend it gets moved and integrated into the paragraph at line 33 or before that paragraph.

**Answer:** Yes, we agree with the reviewer that this paragraph fits better before the last paragraph of the introduction and we moved it there.

**g) p. 2 lines 16-32:** Most of the cited works here are within the past 2 years, however UAVs for atmospheric research have been more widely used for ~10 years. I recommend that the authors provide more details on the pioneering (first) uses of UASs for atmospheric measurements.

**Answer:** Yes, it is true that UAVs were already used for some decades. We inserted the following paragraph to show the pioneering usage of UAVs and included the citations in the

references:

*"From the 1970s on, UAVs were used for atmospheric research, for example for convective processes (Konrad et al., 1970; Rennó and Williams, 1995) and weather forecast (Holland et al., 1992; McGeer and Holland, 1993), as well as for vertical sounding of the planetary boundary layer (Egger et al., 2002; Soddell et al., 2004; Spiess et al., 2007)."*

**h) p. 3 line 20:** Add a statement 'location of instruments is shown in Fig. 1'.

**Answer:** We included the following sentence:

*"An overview about the location of instruments is given in Fig. 1."*

**i) p. 3 line 24 & 27:** Remove references to Fig. 1, seems odd here since the figure does not show the resolution. Seems like odd placements.

**Answer:** We removed the references to Fig. 1 in those two lines.

**j) p. 4 line 14:** Here, the authors discuss night flights. In the next paragraph, it states that the aircraft has permission to fly in the daytime. Did the authors fly at night when there was no permission? Alternatively, if they did get special permission for the night flights, this should be explained so that it is clear the flights were legally conducted.

**Answer:** We agree that this statement is misleading. We exchanged *"daytime"* with *"time of the day"* which makes it clear that day and night is meant.

**k) p. 4 line 30:** What are the specifications for the pressure sensor? This is important to identify the accuracy of the potential temperature calculation.

**Answer:** We included the specification of the pressure sensor as follows:

***"**The used pressure sensor is a MS5611-01BA03 (AMSYS, Mainz, Germany) and is able to resolve an altitude of 10 cm corresponding to a precision of about ±0.02 hPa."*

**l) p. 5 line 12:** Can this method be used to retrieve 'w' as well as u/v? If not, specify that the horizontal wind speed is measured.

**Answer:** No, the vertical wind component cannot be estimated with that method, only the horizontal components. We specified the text:

*"Consequently, in the easiest case the direction of TAS represents the horizontal wind direction and the length of the TAS vector the horizontal wind speed."*

**m) p. 5 line 30 / Fig. 4:** Was the RMSE of the wind speed measurement a function of speed? Specifically, were high or low wind speeds measured more accurately? In Fig. 4, it may be more useful to show errorbars for each data point separately, if the statistics are

robust enough to calculate the RMSE at each speed bin. Similarly, was the RMSE for the tilt angle constantly 0.4 deg at all speeds?

**Answer:** The wind speed estimation is a function of TAS, which is equal to the flight speed under completely calm conditions (no wind). Since the experiment took place outside, this was not totally true (wind speed < 1 m $s^{-1}$). Therefore, a specific flight speed can be assigned to a specific tilt angle, which shows a variability depending on actual atmospheric conditions. The less small-scale turbulence was present the lower the variability of the tilt angle. But this variability was independent on the flight speed. So within the measurement accuracy, it is not possible to determine whether the estimation of low wind speeds is more accurate than higher wind speeds or the other way round. However, the relative error of wind speed estimation is higher for lower than for higher wind speeds, considering a mean TAS error.

Tow sentences were added in the manuscript, the first on p. 5, l. 27 and the second on p. 5, l. 31:

*"While the ground speed was kept constant by the GPS (< ±0.2 m $s^{-1}$), the variability of the assigned tilt angle was dependent on atmospheric conditions."*

*"This mean error of TAS leads to a higher relative error for low wind speeds than for higher wind speeds."*

**n) p. 6 line 7:** What qualifies as 'windy'? Give specifics.

**Answer:** In order to give numbers for windy conditions, we added this to the sentence:

*"During windy conditions (3–5 m $s^{-1}$) the multicopter was hovering for 5 min close to the tower at a distance of approximately 5 m."*

**o) p. 6 line 15:** Since the inlet for the methane measurement was only 30 cm above the propellers, how was it ensured that the measurement was not disturbed by the flow above the spinning propellers? The methane measurement was taken as a 60 s average; during that 60 s, surely the measurement was distorted as air is transported downward by the propellers.

**Answer:** Yes, it is true that during 60 s the air was distorted due to the spinning propellers. Simulations and experiments showed that the air above a multicopter is affected up to 2 m (Haas et al., 2014), but most of the influence is within the first 0.5 m (Alvarado et al., 2017). Unfortunately, Haas et al. (2014) belongs to the grey literature and is not cited in the manuscript.

A sentence was included in the manuscript on p. 6, l.18 and literature was added to the references:

*"Alvarado et al. (2017) experimentally determined a distance of 40–45 cm above the multicopter, where the influence of the rotors to air speed decreases significantly. So, the*

*methane mixing ratio is actually not a point measurement but valid for a volume."*

Reference Haas et al. (2014):

Haas, P. Y., Balistreri, C., Pontelandolfo, P., Triscone, G., Pekoz, H., and Pignatiello, A.: Development of an unmanned aerial vehicle UAV for air quality measurement in urban areas, In 32nd AIAA Applied Aerodynamics Conference, 2014.

**p) p. 6 line 26:** Looking at Fig. 5 (and the standard deviations given on lines 23-24), it is clear that the multicopter does not capture the full range of variability that the sonic anemometer measures. The extrema measured by the tower are much larger (1.5 m/s and 6 m/s) compared to the hexacopter. Presumably the hexacopter measurement is some kind of an average, possibly because the volume the hexacopter takes up is much larger than the sonic measurement volume and the hexacopter has inertia. Have you tried running a smoothing filter (or low-pass filter) over the sonic data to quantify these effects? These effects should be noted in the manuscript, as the wind speed deviation should not be used as a measure of turbulence (since it does not compare favorably, at least here, to the sonic anemometer measurement).

**Answer:** Yes, the multicopter does not capture the full range of variability compared to the anemometer because of inertia. Actually, we used the same 10 s moving average for the anemometer as for the multicopter. To make that clearer, we added this to the sentence on p. 6, line 25:

*"For both time series the 10 s moving average was applied resulting in a RMSE between multicopter and tower of 14.5° and 0.7 m $s^{-1}$, respectively."*

Additionally, we included following sentences at the end of this paragraph to note the effects of inertia:

*"Since the volume of the multicopter is larger compared to the measurement path of the sonic anemometer, the multicopter does not react to the small turbulent elements, the so-called eddies, and therefore cannot capture the full range of wind speed. In addition, the multicopter has inertia due to its weight. Consequently, the wind speed deviations measured by the multicopter should not be used as information about atmospheric turbulence."*

In order to see the standard deviation of multicopter and tower measurements in the plot (Fig. 5) and not only have the numbers in the text, we added colored bands to the time series lines. Accordingly, an explanation is given in the caption:

*"The colored bands around the lines represent the standard deviation of each time series."*

**q) Fig. 6:** To increase readability and for ease of comparison, I suggest averaging the lidar and EC data over the profiles. To convey the variability, error bars could be used.

**Answer:** Indeed, averaging the data makes it easier to understand and the variability is still visible with the error bars. Additionally, we extended the caption of Fig. 6 to:

*"LIDAR and EC station data were averaged over the time the multicopter needed for the profile. Error bars show their standard deviation."*

**r) p. 7 line 8:** Could topography cause the observed wind speeds at the sodar site and multicopter site to be higher? Without a map of the topography, this is difficult to determine.

**Answer:** In order to have an impression of topography from the investigation site, we included contour lines in Fig. 1. Generally, topography as well as different land uses can cause different wind conditions comparing the available instruments. While topography is the predominating reason for west wind situations, during north-east wind, the edge of the forest causes the generation of turbulence leading to spatial differences in wind conditions. Therefore, we included the following sentence (p. 7, l. 9):

*"Besides, during north-easterly winds generation of turbulence is likely at the edge of the forest, which is to the east of the investigation area."*

**s) p. 7 line 22 and Fig. 7:** When was sunset? I suggest adding a vertical line on Fig. 7 denoting sunset time. Also, keep units consistent for CH4 (either ppm or ppb). For the caption of Fig. 7, clarify what the error bars show exactly (standard deviation of what, the 1-min timeseries)?

**Answer:** On that day, sunset was at 19:05 UTC at the investigation site. Since this was about 15 min before our UAV measurements started, the vertical line indicating sunset would be on top of the y-axis. So, we included the time of sunset on p.7, l. 13:

*"In the night between 21 and 22 July 2015, methane measurements were made with the multicopter starting about 15 minutes after sunset (19:05 UTC) and extending over seven hours (Fig. 7)."*

"*ppb*" was replaced by "*ppm*" throughout the manuscript: p. 1, l. 20; p. 7, l. 19, 26, 30; p. 8, l.25f; p. 10, l. 1

In the caption of Fig. 7 the following sentence was added:

*"Error bars show the standard deviation for each measurement averaged over 60 s."*

**t) Fig. 8:** i) I suggest changing this to a two panel plot, one panel each for the methane and one for the potential temperature with separate lines for different profile times. With having all

of the profiles on one plot, it will be much easier to see the change in the profile over time, even the small changes and increase in stabilization. ii) Can error bars be added for each measurement? It may clutter the plot too much, but it is something to consider. iii) It would be better to change potential temperature units to Kelvin, as it is usually presented. iv) Also, please explain in the text why there is a discontinuity at each height where the multicopter hovers. Is it due to the fact that the temperature is evolving over the time it is hovering, or some kind of hysteresis in the sensor?

**Answer:** i) We have looked into this but found that the current layout provides most clarity and least clutter. Since the x-axes have the same range for each time step, we think that changes can be seen easily, better than using six different colors and lines crossing each other.

ii) Error bars were added for methane in Fig. 8.

iii) Unit of potential temperature was changed to Kelvin.

iv) Temperature discontinuity was caused by the spinning of the rotors because they stir the air around the multicopter and not because of hysteresis of the sensor. Reviewer 2 suggested to average potential temperature at hovering levels as it is done for methane as well and we changed the profiles and caption of Fig. 8 accordingly to this suggestion:

*"$T_{pot}$ was averaged at hovering levels and smoothed with a moving average (3 s)."*

**u) p. 7 line 28:** How could the gradients be both intensifying and weakening over time? Please clarify.

**Answer:** With stabilization of the atmosphere a vertical $CH_4$ gradient developed, which was intensifying at first. Due to changing meteorological conditions, on the one hand air was mixed vertically due to a weakening of the stable stratification and on the other hand another air mass was advected due to wind direction change. This led to mixing of $CH_4$ too. Afterwards, meteorological conditions were similar to those before at the beginning of the night and the vertical $CH_4$ gradient could develop again.

For clarification we rewrote the sentence and gave a short explanation, which is addressed in more detail in the manuscript on p. 8, l. 1:

*"Vertical gradients were already visible right after sunset, were intensifying until the measurement at 22:32 UTC, weakening afterwards and then intensifying again at 00:32 UTC. This variability in varying gradients was in agreement with changing meteorological conditions."*

**v) p. 7 line 31:** There was an increase at 50 m as well, it simply was not as large of an increase.

**Answer:** It is true and we removed this sentence and wrote instead:

*"The strongest increase was seen at all heights between 21:32 and 22:32 UTC with 0.25 ppm at 10 m, 0.15 ppm at 25 m, and 0.06 ppm at 50 m."*

**w) p. 8 line 23:** With regard to the statement 'although the multicopter does stir air with its propellers', are there any tests you can do to quantify these effects on the inlet? Measure the flow disturbance at the inlet itself to infer any vertical transport during the 60 sec hovering periods?

**Answer:** Experiments regarding this issue were already done by Alvarado et al. (2017) and Palomaki et al. (2017). Palomaki et al. (2017) used the same hexacopter configuration except with larger propellers (9'' versus 14'') as we in our study leading to an air speed of 0.5 m $s^{-1}$ at 30 cm above the multicopter. Alvarado et al. (2017) found even less influence above 40–45 cm.

For additional information, this was inserted in the manuscript on p. 8, l. 23:

*"Palomaki et al. (2017) demonstrated in an experiment that wind speed at 30 cm above the hexacopter is 0.5 m $s^{-1}$ due to spinning rotors. According to Alvarado et al. (2017) this influence is negligible at a distance of 40–45 cm above the multicopter."*

**x) p. 9 line 8:** Given these values were made using only 5-min of data under a small range of values, the robustness of these statistics is questionable. I suggest adding a qualifying statement here to emphasize these limitations. Also, the RMSE of the wind direction is highly dependent on the wind speed. At low wind speeds (<1 m/s), the RMSE of the wind direction measurement would be much larger.

**Answer:** Yes, it is true that this is rather a qualifying result and not a quantitative one. Since the experiment already had the limitation of < 1 m $s^{-1}$, wind speeds below that cannot be determined.

*"Since the estimated errors were a result of only a 5 min flight, further experiments and comparisons would be necessary to confirm these values. Our experimentally determined relationship between TAS and the tilt angle is only valid for this hexacopter configuration and up to a speed of 6 m $s^{-1}$."*

**y) p. 9 line 13:** This statement should be modified. The vertical wind profiles were not in good agreement. The wind speed from the mulitcopter was systematically larger, and the wind direction was also biased high.

**Answer:** Taking into account the uncertainties of the wind measurements as well as topography, horizontal distance and averaging time, wind estimation is in good agreement from our point of view. We included the statement about the biased results and specified differences:

*"Although the multicopter-based wind estimation was biased, measurements show similar results and the results of the other instruments showed differences too. Wind speed differed up to about 1 m $s^{-1}$ and direction up to 50° above 50 m. Below this height, influences of topography, land use and horizontal distance as well as averaging time were more pronounced and differences larger. Horizontal distance to the multicopter was 370 m for LIDAR and 540 m for SODAR, while they had averaging times of 1 min and 10 min, respectively, compared to the 10 s moving average of the multicopter."*

**z) p. 9 line 16:** Were the differences that Lothon et al (2014) systematically different (biased), or were the differences more scattered (inaccurate)?

**Answer:** The differences Lothon et al. (2014) found were biased dependent on horizontal distance and land use. We change the sentence to:

*„Lothon et al. (2014), for example, found similar biased differences dependent on horizontal distance and land use during the BLLAST campaign."*

**aa) p. 9 line 23:** Should 'in the west' actually be 'to the southwest'?

**Answer:** Looking at Fig. 1, the "Farms" are to the west of the "Methane tower". To avoid ambiguities of the flight locations, we added a sentence at the end of section 2.4:

*"While most of the flights were done above the grassland site south of the EC station as shown in Fig. 1, the flights including methane measurements took place close to the methane tower in the south-east of the investigation area."*

Technical corrections:

**a) p. 3 line 2:** Should this be Sect. 2.2 (not 2.4)?

**Answer:** Sect. 2.2 was added, because this section explains the measurement device and in Sect. 2.4 the measurements themselves are explained.

**b) p. 3 line 9 and p. 4 line 29:** 'at' instead of 'with' 10 Hz.

**Answer:** Corrected as suggested.

**c) p. 4 line 22:** 'approximately' instead of 'approx.'

**Answer:** Changed as suggested.

**d) p. 4 line 23:** Use 'At 50 m length' instead of 'In 50 m height'.

**Answer:** Changed as suggested.

**e) p. 5 line 17:** 'simultaneous' instead of 'simultaneously'

**Answer:** Changed as suggested.

**f) p. 6 line 6:** 'a' instead of 'an'

**Answer:** Changed as suggested.

**g) p. 6 line 7:** 'at' instead of '@'

**Answer:** Changed as suggested.

**h) p. 7 line 29:** Remove 'of these gradients' and 'respectively'

**Answer:** Removed as suggested.

**i) p. 7 line 31:** Remove 'remarkably'

**Answer:** Removed as suggested.

**j) p. 9 line 20:** Change 'is' to 'if'

**Answer:** Corrected as suggested. In addition, "is" was inserted:

*"If this angle is significantly…"*

**k) p. 10 line 11:** Add missing word, 'hence infer dispersion and mixing processes'.

**Answer:** The word "infer" was inserted.

## Reviewer #2

**a) general:** although I am not a native speaker, I think the correct word before naming an altitude is 'at', not 'in' or 'for', e.g. text below Fig. 5, lines 14 and 27 on page 7, etc.

**Answer:** According to your suggestion we changed it in the caption of Fig.5, on page 7 lines 10,14,27,33, page 8 lines 5,10,15 and page 9, line 17.

**b) Page 5 and following:** The procedure to find the relationship between tilt gamma and true airspeed TAS is based on the following assumptions:

1) TAS equals ground speed (measured using GPS) during absent wind (very calm wind, below 1 m/s)

2) TAS and gamma have a linear relation. Thus knowing gamma from attitude measurements leads directly to the TAS.

3) Since the difference between TAS and ground speed equals the wind vector, knowing the attitude / Euler angles allows the calculation of the wind vector (or at least an estimation)

First question addresses assumption #1: what is the mistake done to the TAS-gamma relationship by assuming zero wind during calm wind (1 m/s is not zero)?

**Answer:** Concerning assumption 1: The length of TAS equals the length of the ground vector, but the direction of both vectors is in opposite direction.

As written on p. 5, l. 33ff, the variability of the tilt angle is 0.7° ±0.3° during wind speeds < 1 m/s. Together with the mean error of gamma of ±0.4° in the regression, the maximum absolute error is 0.7° ±0.7° which corresponds to 0.7 m $s^{-1}$ ±0.6 m $s^{-1}$.

Assumption #2: TAS and tilt angle gamma are not in a linear relation, but due to
Seddon, J. M., and S. Newman, 2011: Basic helicopter aerodynamics. 3rd ed., Wiley, 286 pp.,
and
Palomaki et al., 2017, Wind estimation in the lower atmosphere using multi-rotor aircraft, JTECH online: http://journals.ametsoc.org/doi/10.1175/JTECH-D-16-0177.1 (btw this article should be cited anyway),
TASˆ2 = C * tan gamma
Even assuming very small gamma angles, a Taylor series expansion would lead to
TASˆ2 approx C * gamma, and not TAS approx C * gamma !
This explains why the curve in Fig. 4 is not a straight line.

**Answer:** It was not an assumption from us that TAS and gamma have a linear relationship. This was found experimentally with the racetrack flights. This method is widely used for aircraft measurements of the 3D wind vector with turbulence probes (e.g. multi-hole probe). The difference is that an aircraft is flying with a constant true air speed and a varying ground speed dependent on the wind conditions. To counteract these conditions, a lead angle is used. In contrast, a multicopter has a continuous ground speed and varying true air speed; the wind is compensated by changing the tilt angle.

Palomaki et al. (2017) was included in the manuscript (p. 2, l. 28) and references:
*"In addition, Neumann and Bartholomai (2015) and Palomaki et al. (2017) showed that the onboard flight control sensors can be used to derive wind estimates from a multicopter's attitude control data."*

c) How was the wind direction estimated for situations with significant wind speed? Is the simple linear (or squared, see comment b) approach still valid for significant wind speed?

**Answer:** Since the maximum flight speed of the multicopter is about 10 m $s^{-1}$, significant wind would be in the range of 7–8 m $s^{-1}$, which is 70–80 % of the speed. Our experiment to determine the regression function included that speed, but within the 120 m long straight legs

this speed could not be reached. Therefore, the approach is valid up to ~6 m/s and not for significant wind speed. Further tests for significant wind speed were not done yet and for the flights in this manuscript this was not necessary.

d) While the relation between gamma and TAS in Fig. 4 was found for calm wind situations only, the corresponding calibration experiment (race-tracks flights) was performed without the 70 m tube that provides the methane measurements in the following. The tube adds weight and moment of inertia to the multicopter and thus changes the flight mechanics. What / how large is the influence of the tube on the relation between gamma and TAS, and finally on the wind-vector estimation? I see that this aspect is addressed in line 4 on page 9 - but there it is just a statement, not explained or proven.
Of course the autopilot could handle the extra load, but this does not mean that the gamma-TAS relation remains untouched.

**Answer:** Concerning the effect of the tube to the wind estimation, Neumann and Bartholomai (2015) stated that the influence of the payload is negligible regarding the TAS-gamma relationship. Their tests included a payload of 27 % of the takeoff weight. In our case, the additional payload was 30 % at 50 m a.g.l. and was therefore in the same range. Additionally, since the wind data were only used during hovering, no change in payload occurred compared to ascending to the next level.
We included a statement in the manuscript (p.9, l. 4f):
*"A negligible influence of payload was also found by Neumann and Bartholomai (2015)."*

* Chapter 3.2: How much time did the multicopter spend at the three probing altitudes 10, 25 and 50 m?

**Answer:** The multicopter hovered 60 s at each level, which is written on p. 6, l. 15.

* Chapter 3.2 / Fig. 8: The curvature of the blue temperature lines in Fig. 8 is misleading, because it does not represent the vertical temperature profile of atmosphere, but was most likely caused by (all together)
1) non-stationarity of the ABL
2) the change of the multicopter flight mechanics before climbing to the next probing level (thrust) and thus the change of the wind field around the aircraft
3) sensor inertia of the quite slow thermocouple I suggest to use averaged temperature data at the three probing levels only, similar to the CH4 data (green)

**Answer:** We agree with statement 1) and 2), but with a time response better than 1 Hz the thermocouple is not slow and the discontinuities of potential temperature were rather caused by the rotors downwash and drawing air from above, which was mentioned by Reviewer #3

too.

But we agree with averaging the temperature data as for methane and smoothed the profile using a 3 s moving average. This was included in the caption of Fig. 8:

*"$T_{pot}$ was averaged at hovering levels and smoothed with a moving average (3 s)."*

**e) line 29 on page 7**: How is the 'mean concentration of a gradient' defined?

**Answer:** It means that the data at each height were averaged over all measurements. So the mean concentrations at each height are not the same and therefore there is a gradient. For clarification in the text, it was changed to:

*"Mean concentrations averaged over all measurements at each level were 2.091 ppm (10 m), 2.049 ppm (25 m), and 1.976 ppm (50 m)."*

**f) line 30 on page 7:** 'concentrations increased even before sunset' - how can you know? Because line 13 same page: 'starting 15 minutes after sunset'

**Answer:** Since methane measurements were done continuously at the tower, we know that close to the ground the concentration already increased before sunset. We included this explanation as follows:

*"According to the continuous measurements at the tower, the $CH_4$ concentration increased close to the ground even before sunset."*

**g) line 7 on page 8:** 'due to the fact that turbulence was not totally suppressed' - Well, this is more a guess rather than a fact, since turbulence was not measured.

**Answer:** Yes, it is true that turbulence was not measured. But since methane was mixed, vertical exchange was present. To make it clear that this is a guess we changed the sentence to:

*"The results indicated a developing surface layer up to 25 m a.g.l. where methane accumulated, but exchange with air above was not completely inhibited likely due to the fact that turbulence was not totally suppressed."*

**h) line 22ff on page 9:** You could visualise the mulitcopter downwash and quantify the downwash area using smoke. We did this - really easy to do and impressive.

**Answer:** Thank you for this suggestion, we will try it out.

**i) section 3.2 and line 27ff on page 9**: the methane data interpretation depends strongly on the accuracy of the methane concentration measurement, which is not addressed in the article. How accurate is the CRD spectrometer? See also missing error bars in Fig. 8 for additional statistical uncertainty.

**Answer:** Yes, it is right that there is no information about the accuracy of the CRD spectrometer. We included this information in section 2.1 where the instrument was introduced. Error bars were included in Fig. 8.

*"Methane mixing ratios were determined using a cavity ring down (CRD) spectrometer (G2508, Picarro Inc., Santa Clara, CA, USA) with an accuracy of < 0.007 ppm."*

**j) Fig. 6 and line 13ff on page 9:** it seems that the lidar wind direction at 9:00 UTC was corrupt due to very low wind speed. Same for all lidar data below 25 m. I looks like the lidar did not deliver reliable data at all under these conditions, and that this has nothing to do with horizontal separation from the sodar etc. This should be mentioned.

**Answer:** Yes, the determination of wind direction is more difficult when wind speed is low. But this has nothing to do with height. At 9:00 UTC, wind speed measured by the LIDAR was even lower at around 50 m leading to higher variability in direction. At 9:30 UTC, wind speed was higher and wind direction variability was lower. For clarity, we included the following sentence at the end of this paragraph:

*"In addition, low wind speeds (< 1 m $s^{-1}$) lead to high variability in wind direction as seen for LIDAR data."*

Due to the insertion of this sentence, the following two sentences were swapped and modified as follows:

*"This is because then the wind is not well coupled to the meso-scale flow, which is often leading to variable wind directions (Anfossi et al., 2005, Mahrt, 2010). The same is true for multicopter-based wind direction at 10 m during the nighttime flights, which mainly occurred during wind speeds of less than 2 m $s^{-1}$."*

**k) Fig. 7:** for most data points the error bars are missing (since data points are a result of averaging it should be easy to add error bars)

**Answer:** In Fig. 7, the error bars are not missing, they are sometimes just not larger than the size of the data point. This includes a standard deviation of 10 ppb or less. Therefore, an explanation was inserted in the caption of Fig. 7:

*"Error bars show the standard deviation for each measurement averaged over 60 s. A standard deviation of 0.01 ppm or less cannot be shown because the size of the data point exceeds the error bar."*

**l) Fig. 8:** Since the data points (at least the CH4 concentration) are a result of averaging it would be easy to add error bars. This would give better confidence, or rather would help to see the significance of the concentration gradient described in the text, respectively.

**Answer:** Error bars were included in Fig. 8. As for Fig. 7, a standard deviation of 10 ppb or less cannot be represented and therefore error bars are not visible. We added two sentences in the caption of Fig. 8:

*"Error bars of methane concentration show the standard deviation for each measurement averaged over 60 s. A standard deviation of 0.01 ppm or less cannot be shown because the size of the data point exceeds the error bar."*

**m) Fig. 9:** How were the errors calculated? What do the small circles represent?

**Answer:** The boxplots in Fig. 9 represent the variability of wind speed and direction at each level during the hovering time of 60 s. The caption of Fig. 9 was adapted as follows:

*"Figure 9: Variability of wind direction (left) and speed (right) during 60 s hovering at 10, 25 and 50 m a.g.l. for flights between 19:32 UTC and 00:32 UTC in the night 21 to 22 July 2015. The blue box contains 50 % of the data and represents the interquartile range with the median as a black line. The dashed lines show maximum and minimum values in case those values are within the 1.5 interquartile range. Values outside this range (outliers) are represented with circles."*

## Reviewer #3

First, based on the placement of the temperature and humidity sensors (on the arm of the multicoptor below one rotor; Fig. 1), it is very likely that these meteorological measurements were negatively impacted by rotor-wash. Indeed, the discontinuities in the potential temperature profiles at UAV sampling locations (Fig. 8) support this idea. I suggest placing the meteorological sensors closer to the methane inlet and away from the rotors. At the very least, this flaw in the method should be openly discussed and addressed in future studies. The authors should also comment on why the humidity data obtained from this sensor was not presented. Ideally, the authors could demonstrate using laboratory tests that the current flying geometry and sampling strategies do not adversely affect the either the methane measurements or the wind estimates.

**Answer:** Yes, the rotor downwash has an impact on the temperature and humidity sensors, but this position was chosen to ensure a continuous flow to make the sensors faster. To address this, we included a sentence in the discussion (p. 9, l. 27):

*"Since the thermocouple was placed below a rotor, discontinuities were found while hovering; the temperature measurement is rather representative for the volume around the multicopter than for a point. But this ensured a continuous flow around the sensor, which increased its*

*response time. For analysis, temperature was averaged for hovering at each level during the methane measurements."*

The humidity data were not shown in this study because the used SHT75 sensor was not fast enough for vertical profiles and always showed a hysteresis. Although the hovering time was long enough for the sensor to adapt to surrounding conditions during the methane measurements, humidity data were not shown. This was because this sensor is not appropriate for this kind of UAV-based measurements.

Concerning the suggested laboratory tests with regard to effects of the flying geometry and sampling strategy on methane measurements and wind estimates, this was already shown in other studies and addressed in this revision.
For methane measurements, we would like to refer to the comments o) and w) of Reviewer #1 and for wind estimation to comment c) of Reviewer #2.

The interpretation of the methane concentration gradients rely heavily on the interpretation of the meteorological conditions and changes in the surface layer with time. As a result, it would be helpful for figures 7 and 8 to show the local time, as well as UTC time.
**Answer:** Yes, we agree with this. In the manuscript, we included the sentence (p. 6, l. 19):
*"Time is given in UTC which corresponds to CEST-2."*

In addition, we stated local time in the caption of Fig. 7 and 8 explicitly:
Fig. 7: *"Local time (CEST) is UTC+2."*
Fig. 8: *"This corresponds to: 21:32 CEST to 02:32 CEST (UTC+2)."*

The discussion on L25-30 is difficult to follow and should be re-written.
**Answer:** Since the page number for this comment was not given, it was not clear to us which discussion was meant by the Reviewer. Therefore, unfortunately, we could not address it.

Finally, as noted in the manuscript, a more powerful UAV with a larger payload would enable longer profiles by ground-based gas spectrometer. Given a UAV with a larger payload, could the authors comment on what is the maximum altitude that could be reasonably sampled using this method, either due to prolonged residence time in the tubing, flow restrictions or other logistical concerns?
**Answer:** From our point of view, it is difficult to give a maximum altitude, which is possible with this method. We would rather suggest the other way round. (1) What is the altitude you want to reach, (2) how long you want to sample at each height and (3) at how many heights?

From (1) you know the length of your tube. The residence time in the tube is dependent on the pump in the gas analyzer and the diameter of the tube. This defines the possible flow rate and the sampling time at each height. Is (1) not reachable, a higher payload is needed or an adaptation of (2). Depending on the payload the possible flight time defines (3). In addition, it has to be highlighted that the material of the tube should not react with the gas of interest. Therefore, inert gases as methane are preferable to measure with this method.
From other methane measurements during the campaign we know that it is possible to use a 1/4 inch Teflon tube with a length of 140 m. But the weight of this tube is about 2 kg, which would have been too heavy for our hexacopter.
So, the existing parameters and limitations affect the possible reachable altitude for each individual application. Therefore, no maximum altitude was stated in the manuscript.

## Further technical corrections by authors

a) “LiDAR” was replaced by “LIDAR” throughout the text
b) p. 2, l. 19: “size distribution” instead of “size distributions”
c) p. 3, l. 7: “TERrestrial” instead of “TERrestrail”
d) p. 3, l. 20: “Mauder et al., 2013” instead of “Mauder et al., 2014”
e) p. 4, l. 17: Comma was inserted

## Additional literature included in the references

Alvarado, M., Gonzales, F., Erskine, P., Cliff, D. and Heuff, D.: A Methodology to Monitor Airborne $PM_{10}$ Dust Particles Using a Small Unmanned Aerial Vehicle, Sensors, 17, 343, doi:10.3390/s17020343, 2017.

Banta, R. M., Pichugina, Y. L., Kelley, N. D., Hardesty, R. M., and Brewer, W. A.: Wind energy meteorology: Insight into wind properties in the turbine-rotor layer of the atmosphere from high-resolution Doppler lidar, Bull. Amer. Meteorol. Soc., 94, 883-902, doi:http://dx.doi.org/10.1175/BAMS-D-11-00057.1, 2013.

Egger, J., Bajrachaya, S., Heinrich, R., Kolb, P., Lämmlein, S., Mech, M., Reuder, J., Schäper, W., Shakya, P., Schween, J., and Wendt, H.: Diurnal winds in the Himalayan Kali Gandaki valley. Part III: Remotely piloted aircraft soundings, Mon. Weather Rev, 130(8), 2042-2058, 2002.

Hammann, E., Behrendt, A., Le Mounier, F., and Wulfmeyer, V.: Temperature profiling of the atmospheric boundary layer with rotational Raman lidar during the HD(CP)2 Observational Prototype Experiment, Atmos. Chem. Phys., 15, 2867-2881, doi:10.5194/acp-15-2867-2015, 2015.

Holland G. J., McGeer T., and Youngren H.: Autonomous aerosondes for economical atmospheric soundings anywhere on the globe, Bull. Amer. Meteorol. Soc., 73(12), 1987-1998, 1992.

McGeer T., and Holland G.: Small autonomous aircraft for economical oceanographic observations on a wide scale, Oceanography, 6(3), 129-135, 1993.

Palomaki, R. T., Rose, N. T., van den Bossche, M., Sherman, T., J., and De Wekker, S. F. J.: Wind Estimation in the Lower Atmosphere Using Multirotor Aircraft, Atmos. Oceanic Technol., doi:10.1175/JTECH-D-16-0177.1, in press, 2017.

Rennó N. O., and Williams E. R.: Quasi-lagrangian measurements in convective boundary layer plumes and their implications for the calculation of cape. Mon. Weather Rev, 123(9): 2733-2742, 1995.

Soddell, J. R., McGuffie, K., and Holland, G. J.: Intercomparison of atmospheric soundings from the aerosonde and radiosondes, J. Appl. Meteor. Climatol., 43(9), 1260-1269, 2004.

Spiess T., Bange J., Buschmann M., and Vörsmann P.: First application of the meteorological Mini-UAV “M2AV”, Meteorol. Z., 16(2), 159-169, doi:10.1127/0941-2948/2007/0195, 2007.

## Updated Figures and captions

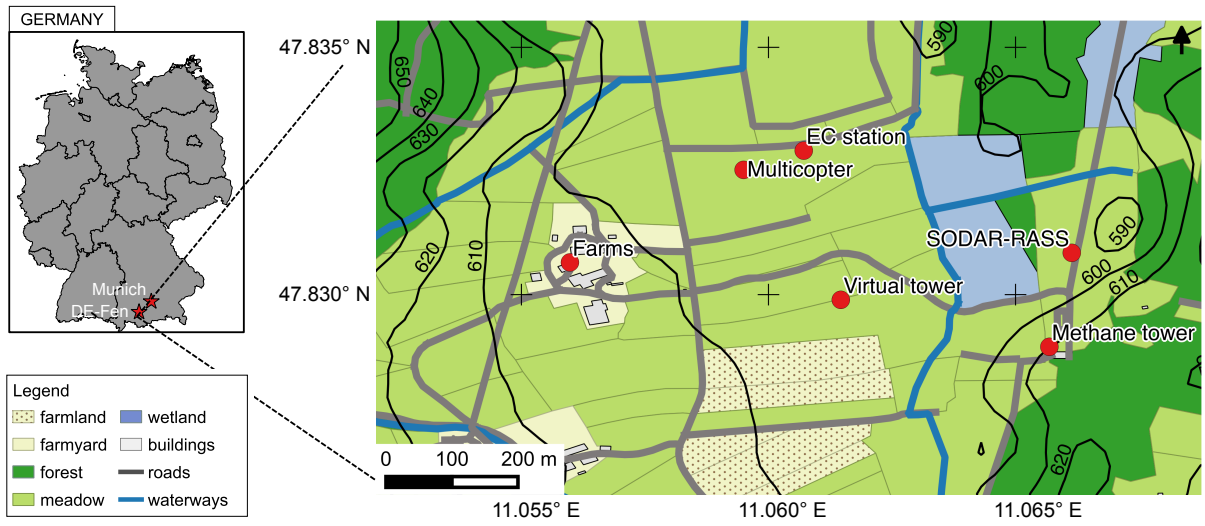


**Figure 1: Measurement site DE-Fen, Germany, with land use and ground-based instrumentation important for this study during the ScaleX campaign 2015. Contour lines stand for altitude (m) above sea level (QGIS, OpenStreetMap).**

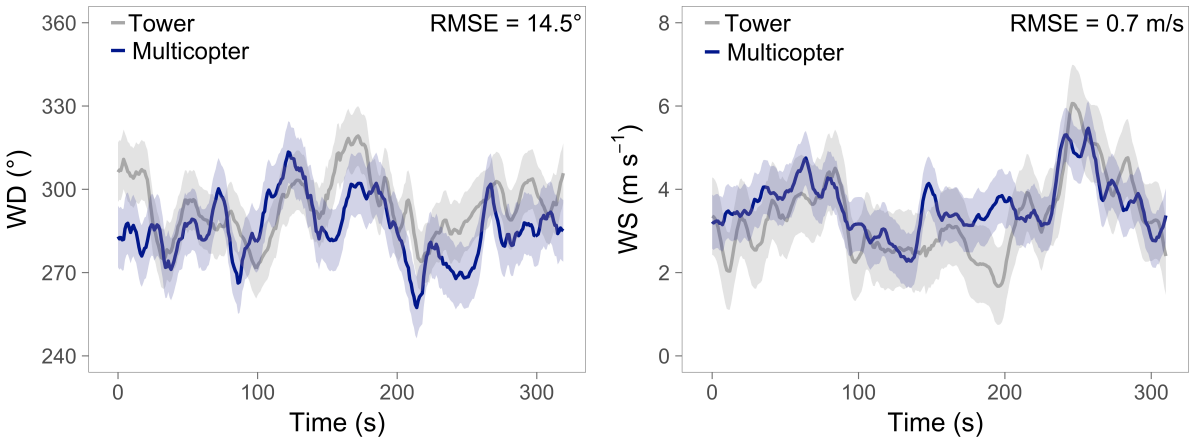


**Figure 5: Wind direction (WD) and speed (WS) comparison between tower (grey) and multicopter (blue) at 9 m a.g.l. over 5 min. The colored bands around the lines represent the standard deviation of each time series.**

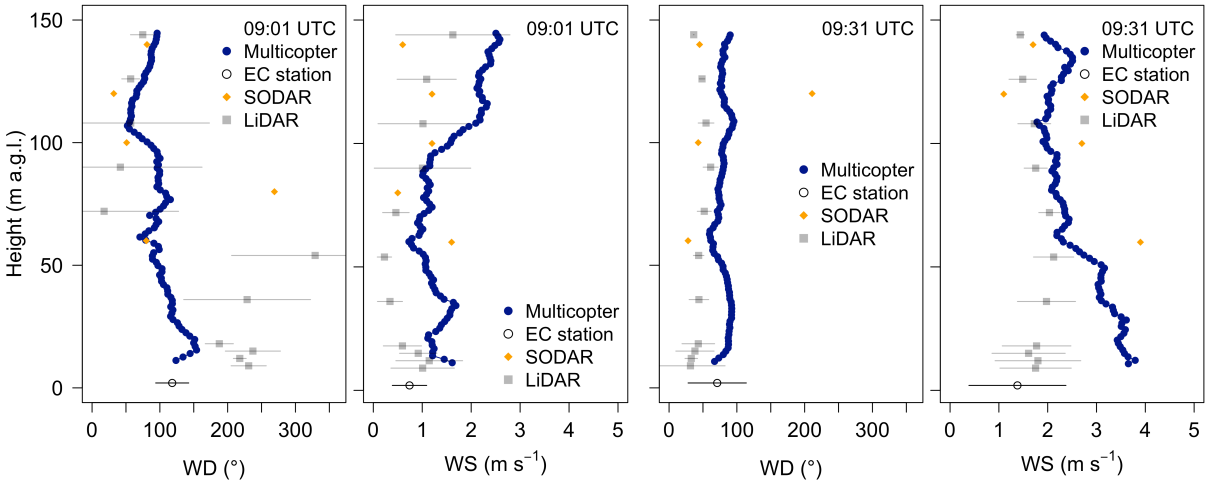


**Figure 6: Wind direction and speed profiles during two different flights: 09:01 UTC (left panels) and 09:31 UTC (right panels) on 15 July 2015. The blue profiles show multicopter data, dark grey circles represent EC station data, light grey squares LIDAR data and orange squares SODAR data. LIDAR and EC station data were averaged over the time the multicopter needed for the profile. Error bars show their standard deviation.**

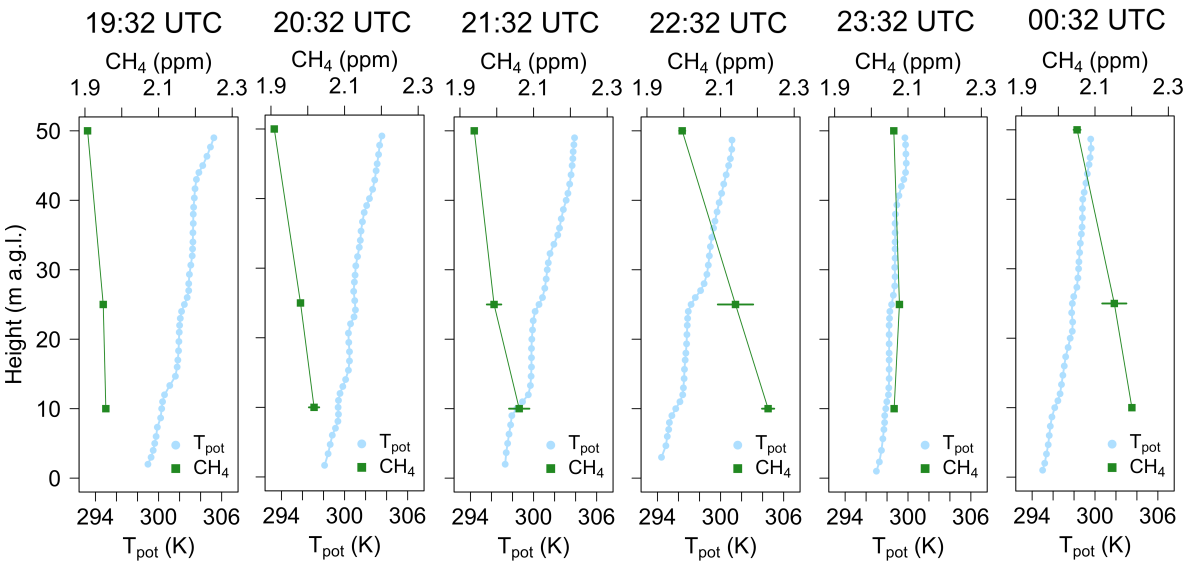


**Figure 8: Vertical potential temperature ($T_{pot}$) profiles in blue and methane concentrations in green over six hours from 19:32 UTC (left) to 00:32 UTC (right) in the night 21 to 22 July 2015. This corresponds to: 21:32 CEST to 02:32 CEST (UTC+2). Air temperature was measured with the thermocouple (ascent data only) and $T_{pot}$ was calculated with the onboard pressure data from the autopilot. $T_{pot}$ was averaged at hovering levels and smoothed with a moving average (3 s). Error bars of methane concentration show the standard deviation for each measurement averaged over 60 s. A standard deviation of 0.01 ppm or less cannot be shown because the size of the data point exceeds the error bar.**

# Simultaneous multicopter-based air sampling and sensing of meteorological variables

Caroline Brosy[1], Karina Krampf[1], Matthias Zeeman[1], Benjamin Wolf[1], Wolfgang Junkermann[1], Klaus Schäfer[1], Stefan Emeis[1], Harald Kunstmann[1,2]

[1]Institute of Meteorology and Climate Research (IMK-IFU), Karlsruhe Institute of Technology, Garmisch-Partenkirchen, 82467, Germany
[2]Institute of Geography, University of Augsburg, Augsburg, 86159, Germany

*Correspondence to*: Caroline Brosy (caroline.brosy@kit.edu)

**Abstract.** The state and composition of the lowest part of the planetary boundary layer (PBL), i.e., the atmospheric surface layer (SL), reflects the interactions of external forcing, land surface, vegetation, human influence and the atmosphere. Vertical profiles of atmospheric variables in the SL at high spatial (meters) and temporal (1 Hz and better) resolution increase our understanding of these interactions, but are still challenging to measure appropriately. Traditional ground-based observations include towers that often cover only few measurement heights on a fixed location. At the same time, most remote sensing techniques and aircraft measurements have limitations to achieve sufficient detail close to the ground (up to 50 m). Vertical and horizontal transects of the PBL can be complemented by unmanned aerial vehicles (UAV). Our aim in this case study is to assess the use of a multicopter-type UAV for the spatial sampling of air and simultaneously the sensing of meteorological variables for the study of the surface exchange processes. To this end, a UAV was equipped with onboard air temperature and humidity sensors, while wind conditions were determined from the UAV's flight control sensors. Further, the UAV was used to systematically change the location of a sample inlet connected to a sample tube, allowing the observation of methane abundance using a ground-based analyzer. Vertical methane gradients of about 0.3 ppm were found during stable atmospheric conditions. Our results showed that both methane and meteorological conditions were in agreement with other observations at the site during the ScaleX-2015 campaign. The multicopter-type UAV was capable of simultaneous in situ sensing of meteorological state variables and sampling of air up to 50 m above the surface, which extended the vertical profile height of existing tower-based infrastructure by a factor of five.

## 1 Introduction

The planetary boundary layer (PBL) is the lowest part of the atmosphere directly influenced by the Earth's surface and reflects interactions between land surface, vegetation, human activities and the atmosphere (Stull, 1988). Since mixing processes and transport or the lack of those affect trace gas and aerosol distributions in the atmosphere on all scales, vertical profiles provide more detailed information which have to be accounted for when dealing with emission and flux estimations (Worden et al., 2012).

Well-known in situ platforms for the measurement of vertical profiles of atmospheric variables in the PBL are towers, (tethered) balloons and radiosondes (Konrad et al., 1970). The operation of towers is fixed to a certain location and the vertical information is limited to the height of the tower as well as to discrete levels at the tower. However, towers provide continuous recording of the investigated variables and are routinely used (e.g. Sasakawa et al., 2010; Wang et al., 2013; Andrews et al., 2014). With radiosondes, balloons or kites, information of meteorological conditions can be acquired for an extended vertical range, but these systems are expensive and the location of the vertical profiles is dependent on atmospheric conditions. Nevertheless, mobile and temporary applications are possible. Research aircraft and satellites cover large areas in the range of kilometers within a short time span, but their operation close to the ground is still challenging (Velasco et al., 2008; Martin et al., 2011). Considering ground-based remote sensing methods, data of vertical profiles from low altitudes up to about 50 m above ground level (a.g.l.) are hardly usable (e.g. acoustic instruments), but possible with LIDARs applying certain scan patterns with low elevation angles at the position of such an instrument (Emeis, et al., 2009; Banta et al., 2013; Korhonen et al., 2014; Hammann et al., 2015).

From the 1970s on, UAVs were used for atmospheric research, for example for convective processes (Konrad et al., 1970; Rennó and Williams, 1995) and weather forecast (Holland et al., 1992; McGeer and Holland, 1993), as well as for vertical sounding of the planetary boundary layer (Egger et al., 2002; Soddell et al., 2004; Spiess et al., 2007). In recent years, unmanned aerial vehicles (UAVs) became increasingly used as flying platforms for measurements in atmospheric research for both vertical and horizontal applications (Villa et al., 2016). Martin et al. (2011) demonstrated the utilization of fixed-wing UAVs for measurements of meteorological variables, i.e. air temperature, humidity and wind, up to 1600 m above ground level (a.g.l.). In addition, de Boer et al. (2016) implemented radiation and aerosol size distributions sensors, Altstädter et al. (2015) focused on ultrafine particles and Båserud et al. (2016) showed the possibility of turbulence measurements. Nathan et al. (2015) measured methane with an in situ sensor flying around a compressor station to calculate its emissions. The importance of knowing both meteorological conditions and methane (or aerosols, particulate matter, etc.) was highlighted in previous studies (e.g. Bamberger et al., 2014; Mathieu et al., 2015). Fixed-wing systems can cover a vertical and horizontal range of several kilometers and therefore, they are suitable for investigations throughout the boundary layer. Multicopters offer flexible maneuverability at low flight speed and the possibility of hovering (i.e. no horizontal movement). Their applications include meteorological and air quality measurements, e.g. particulate matter (Alvarado et al., 2015) or air samples for analyses of chemical composition (Chang et al. 2016), but on a smaller scale of several hundreds of meters. In addition, Neumann and Bartholomai (2015) and Palomaki et al. (2017) showed that the onboard flight control sensors can be used to derive wind estimates from a multicopter's attitude control data. Although small and lightweight methane sensors are available (Berman et al., 2012; Khan et al., 2012), current model multicopters with a takeoff weight below 5 kg still require further miniaturization of the sensors. As a consequence, mobile investigations of vertically resolved profiles of greenhouse gases in combination with information about atmospheric state variables are not conventionally applied yet.

Methane ($CH_4$) is the second most important greenhouse gas with regard to global warming and has a global warming potential 20 times that of carbon dioxide (Forster et al., 2007). Its current concentration is more than twice as much as before preindustrial times (Kirschke et al., 2013; Saunois et al., 2016). While the global budget is well known, this is not the case for regional to local scales, especially vertical distributions (Dlugokencky et al., 2011). Using tethered balloons, Choularton et al. (1995), Beswick et al. (1998) and Stieger et al. (2015) investigated the vertical methane distribution within the nocturnal boundary layer (NBL) by pulling up a sampling tube.

In this case study we aim to assess the feasibility of a multicopter-type UAV approach to detach methane and meteorological measurements at a tower by pulling up a tube with a multicopter weighing below 5 kg. Both methane and atmospheric state are important to analyze the vertical methane distribution focusing on stable atmospheric conditions above a typical agricultural setting in the foothills of the Bavarian Alps. The nighttime is of particular interest because turbulent mixing is low and vertical methane gradients can develop.

## 2 Methodology

### 2.1 Site description and instrumentation

The first experiments with our multicopter took place at the measurement site Fendt (DE-Fen) of the TERENO-preAlpine (TERrestrial ENvironmental Observatory) observatory (Zacharias et al., 2011) during the ScaleX campaign (Wolf et al., 2016, in press) in June and July 2015. This intensive campaign aimed to address atmosphere-land surface interactions across different scales with both measurements and modeling. As a long-term TERENO site, DE-Fen is equipped with automated instrumentation and continuous data availability already for several years. During ScaleX, measurements of energy, water and greenhouse gas fluxes were extended in time and spatial resolution to investigate spatial patterns and vertical gradients to obtain three-dimensional and more detailed information.

DE-Fen (47.832 °N, 11.062 °E, 600 m above sea level (a.s.l.)) is located in a north-south oriented valley in the foothills of the Bavarian Alps in southern Germany (Fig. 1). While the surface is relatively flat towards the east about 300 m to the west a steep forested slope of about 100 to 130 m borders the grassland in the valley. Thus, orographical winds and diurnal wind systems favor northerly and southerly directions with occasional easterly or northeasterly components. Westerly winds are normally associated with orographic turbulence. Prevailing land use is grassland with sporadic croplands. Further details on climate characteristics of the region can be found in Kunstmann et al. (2004, 2006).

The site is equipped, among other instruments, with a permanent eddy-covariance (EC) station for carbon dioxide, water vapor and energy flux measurements (Mauder et al., 2013; Zeeman et al., 2017). An overview about the location of instruments is given in Fig. 1. During the campaign, a radio acoustic sounding system (SODAR-RASS, Metek GmbH, Elmshorn, Germany) was installed on the east side of the area. The SODAR-RASS consists of a SODAR for the wind measurement with an acoustic signal and two RADAR antennas for measurements of vertical profiles of air temperature (Emeis et al., 2009). The temporal resolution is 10 min with a range between 40 m to 650 m a.g.l. and a vertical resolution of

20 m. In addition, vertical profiles of wind direction and speed were determined at the intercept of three simultaneously scanning Doppler wind-LIDAR systems (model Stream Line, Halo Photonics Ltd, Worcester, UK) as a so-called 'virtual tower', in 1 min and 18 m intervals and up to approximately 800 m a.s.l.. Methane mixing ratios were determined using a cavity ring down (CRD) spectrometer (G2508, Picarro Inc., Santa Clara, CA, USA) with an accuracy of < 0.007 ppm. The instrument was installed close to a 10 m tower equipped with wind speed and direction measurements (CSAT3, Campbell Scientific Ltd., Bremen, Germany and WindMaster 3D, Gill Instruments, Lymington, Hampshire, UK) and sample air inlets at 1, 5 and 10 m height. The three sampling lines (stainless steel, 3.2 mm outer diameter, 1.2 mm inner diameter) were flushed continuously with ambient air and a custom built system of solenoid valves connected one sampling line to the CRD spectrometer every 75 s. Those measurements were complemented with UAV-based measurements being explained in Sect. 2.2 and 2.4.

**2.2 Multicopter and its instrumentation**

The multicopter used in this study was a commercially available hexacopter DJI F550 Flame Wheel (DJI Innovations, Shenzhen, China) with dimensions of 55 cm x 55 cm x 30 cm and a frame weight of 1.3 kg including motors, propellers, autopilot and electronics (Fig. 2). It was equipped with a Pixhawk (3DR, Berkley, USA) autopilot for stabilized and autonomous flights. The autopilot contains a 3D accelerometer, gyroscope, magnetometer and barometer for position control as well as an external GPS (LEA-6 u-blox 6, u-blox, Thalwil, Switzerland) for autonomous flying. All data were logged onboard, attitude angles as well as motor output at 10 Hz, the accelerometer and gyroscope data at 50 Hz and GPS at 5 Hz. Additionally, a remote receiver was installed onboard for manual flying with remote control. The takeoff weight of 2 kg led to a flying time of approximately 10 min with a ground speed of 5 m $s^{-1}$. In case of a communication loss of the remote control, GPS signal or low battery status a pre-programmed fail-safe mode took over the control and initiated the landing. The open-source software Mission Planner was used for ground control to transmit and display important flight data (e.g. height, horizontal and vertical speed, battery capacity, position) during the flights. For night flights, bright LEDs were mounted on the landing gear of the multicopter for visibility and the identification of its orientation.

This kind of UAV with a weight below 5 kg was chosen to fly with general flight permission from the Bavarian aviation authority, independent on area, altitude above ground and time of the day in the uncontrolled air space.

For vertical methane investigations close to the tower, a 40 cm long aluminum tube (3.2 mm outer diameter, 1.2 mm inner diameter) was installed on the multicopter with the inlet about 30 cm above the propellers. This was attached airtight to an additional sampling line (PTFE, 3.2 mm outer diameter, 2 mm inner diameter, 70 m long) and was connecting the CRD spectrometer and the multicopter. The 70 m sample line was flushed at a flow rate of 350 sccm $min^{-1}$ (calibrated for 0 °C and 1013.25 hPa) of which 200 sccm $min^{-1}$ were drawn by the CRD analyzer. This resulted in a residence time of approximately 38 s in the tube. At 50 m length, the tube was an additional payload of 650 g. Thus, the maximum ascent height was limited by the payload capacity of the multicopter.

A fast thermocouple was installed for high time resolution air temperature measurements. The used thermocouple was a butt welded type K (CHROMEGA®/ALOMEGA® CHAL-003, OMEGA, Stamford, CT, USA), one wire chromium nickel alloy and the other constantan, both with a diameter of 0.08 mm. Its measurement range was 0 ° to 60 °C with an output voltage of 50 mV per °C. The response time was better than 1 Hz in calm air with an accuracy of ±0.1 °C. Calibration against a reference thermometer was done in the lab. Data were logged at 10 Hz. These data were also used together with pressure data from the autopilot for potential temperature ($T_{pot}$) calculations to get information about the stability of the atmosphere. The used pressure sensor is a MS5611-01BA03 (AMSYS, Mainz, Germany) and is able to resolve an altitude of 10 cm corresponding to a precision of about ±0.02 hPa.

### 2.3 Wind estimation

Multicopters move through the air by setting a tilt angle ($\gamma$) towards the flying direction with the magnitude of tilt angle roughly proportional to speed. This angle is also changing for compensation of wind variations during the flight. Therefore, without using an additional sensor for wind measurements, estimation of both horizontal wind speed and direction was possible with onboard sensors for the vehicle's attitude control by measuring the pitch (for- and backwards), roll (left and right) and yaw (orientation to north) angles. In contrast to an aircraft, which is controlled by setting a true air speed, a multicopter is flying with a given ground speed resulting in a varying true air speed.

This relationship is shown in the wind triangle (Fig. 3). The ground (G) vector represents the speed and direction of the multicopter's movement determined by the GPS, while the true air speed (TAS) vector represents for the actual speed and direction the multicopter is heading to. The deviation of G and TAS is caused by the wind. Assuming hovering, the tilt angle is only a result of the wind and the TAS vector is contrary to the ground vector. Consequently, in the easiest case the direction of TAS represents the horizontal wind direction and the length of the TAS vector the horizontal wind speed.

Equations applied for the wind calculation are based on Neumann and Bartholomai (2015) and explained in detail there. In this study, only vertical flights were investigated. First, the multicopter's tilt angle $\gamma$ was calculated from roll and pitch angles and then projected to the xy-plane, which results in the true air speed vector. Then, its direction was calculated relative to the viewing direction of the multicopter (yaw angle ($\psi$)) and is given by the angle $\lambda$. TAS direction and simultaneous wind direction was determined by the sum of $\psi$ and $\lambda$ in case the TAS vector is on the right side of the viewing direction ($[\psi, \psi + 180°]$). In the other case, this sum was subtracted from 360° and in both cases the result has to be within 0° and 360°. Finally, the calculated tilt angle was inserted into a regression function to get the corresponding true air speed. The length of the TAS vector represents the wind speed.

Neumann and Bartholomai (2015) used wind tunnel experiments to determine the regression function. In contrast, in our approach the length of the TAS vector was determined by relating tilt angles to specific true air speeds during different flight experiments. The assumption was that without wind the true air speed corresponds to the flight speed measured with the GPS (GPS speed or ground speed), which has an accuracy of 0.1 m $s^{-1}$. The multicopter's tilt angle was calculated by using pitch and roll angles. Their accuracy was better than 0.1°. Using racetrack flights, the regression function was experimentally

determined during calm wind conditions with wind speeds below 1 m $s^{-1}$. The track had a length of 120 m and had been flown six times on average for several ground speeds between 2 m $s^{-1}$ and 8 m $s^{-1}$. While the ground speed was kept constant by the GPS (< ±0.2 m $s^{-1}$), the variability of the assigned tilt angle was dependent on atmospheric conditions. To avoid an offset in the regression function the multicopter was balanced out. The resulting regression function is shown in Fig. 4 with the following Eq. (1):

$$TAS = 0.9743 * \gamma^{0.8817} \quad (1)$$

The root-mean-square-error (RMSE) of TAS determination was ±0.3 m $s^{-1}$. Based on this error for TAS, the RMSE of the tilt angle was ±0.4°, which is similar to the one of Neumann and Bartholomai (2015). This mean error of TAS leads to a higher relative error for low wind speeds than for higher wind speeds.

With this equation, horizontal wind speed and wind direction were estimated from 1 Hz data and were averaged with a moving window over 10 s for further smoothing. To determine the inaccuracy caused by a wind speed up to 1 m $s^{-1}$ during the experimental flights, the variability of the tilt angle was analyzed during hovering under calm wind conditions (<1 m $s^{-1}$). This led to an uncertainty of 0.7° ±0.3° corresponding to a true air speed of 0.7 m $s^{-1}$ ±0.3 m $s^{-1}$, which resulted in an overall accuracy of TAS estimation of 0.7 m $s^{-1}$ ±0.6 m $s^{-1}$.

### 2.4 Flight strategies

To demonstrate the functionality of the wind estimation based on the attitude control sensors of the multicopter, a comparison was done to a 3D ultrasonic anemometer (uSonic3, Metek GmbH, Elmshorn, Germany) installed at a 9 m tower having an accuracy of 0.1 m $s^{-1}$ and 2° at 5 m $s^{-1}$, respectively. During windy conditions (3–5 m $s^{-1}$) the multicopter was hovering for 5 min close to the tower at a distance of approximately 5 m. This horizontal distance as well as the 9 m height of the measurements ensured that the multicopter's downwash neither had an influence on the multicopter itself nor on the anemometer. For calm wind conditions, influences of the downwash were detected up to 5–6 m a.g.l.

In addition, vertical wind profiles were compared to other instruments such as LIDAR and SODAR. The EC station was used as continuous time series information close to the ground. Reaching a height of 150 m a.g.l. with the multicopter, the range comparable to other instruments was about 100 m. For these flights, the vertical speed was set to 1.5 m $s^{-1}$.

For methane measurements, the additional sampling line was attached to the multicopter and the spectrometer and was raised up to heights of 10, 25 and 50 m a.g.l. A hover time of 60 s at each level was included to get an averaged value. The pattern was repeated every 15 min. This led to a rotation of 5 min measurements with the multicopter and 10 min measurements at the tower at 1 m and 10 m a.g.l. For analysis, only the ascent data were used from the flights because there was no hovering during the descent. In addition, this strategy ensured that the multicopter did not mix the air before flying through. Alvarado et al. (2017) experimentally determined a distance of 40–45 cm above the multicopter, where the influence of the rotors to air speed decreases significantly. So, the methane mixing ratio is actually not a point measurement but valid for a volume. While most of the flights were done above the grassland site south-west of the EC station as shown in Fig. 1, the flights including methane measurements took place close to the methane tower in the south-east of the investigation area.

Time is given in UTC which corresponds to CEST-2.

## 3 Results

### 3.1 Wind estimation

Information about the accuracy of the wind estimation was determined while hovering next to an ultrasonic anemometer with a distance of about 5 m (Fig. 5). The multicopter derived wind direction showed a standard deviation of ±11.1° and ±0.7 m $s^{-1}$ for wind speed within a hovering time of 5 min. During the same time, the anemometer's wind direction varied by ±10.6° and wind speed by ±1 m $s^{-1}$. The difference between the multicopter and tower measurements both averaged over 5 min was 7.7° and 0.3 m $s^{-1}$. For both time series the 10 s moving average was applied resulting in a RMSE between multicopter and tower of 14.5° and 0.7 m $s^{-1}$, respectively. Both changes in wind speed and direction could be captured by the multicopter. The highest deviation was between 150 s and 200 s with differences of about 30° and 2 m $s^{-1}$, respectively (see Fig. 5). Since the volume of the multicopter is larger compared to the measurement path of the sonic anemometer, the multicopter does not react to the small turbulent elements, the so-called eddies, and therefore cannot capture the full range of wind speed. In addition, the multicopter has inertia due to its weight. Consequently, the wind speed deviations measured by the multicopter should not be used as information about atmospheric turbulence.

In addition to the side-by-side measurements, wind estimation from vertical profiles was compared to LIDAR and SODAR measurements as well as EC station data for near ground information (Fig. 6). Both LIDAR and EC station data (both 1 min time resolution) are shown for the time around the vertical profiles of the multicopter (~4 min). The SODAR had a temporal resolution of 10 min, so only one value was available at each height. Wind direction and speed of the UAV data were in good agreement with the recordings of the different instruments. During the flights at 09:01 UTC and 09:31 UTC, wind direction was mainly from north to east with an increasing wind speed over time. For the first flight, spatial and temporal averages of multicopter, SODAR and EC station were in agreement within 20–30° and a standard deviation of about ±20° for wind direction. LIDAR data showed higher variability than other measurements but above 100 m data were in the same range. Wind speed for all instruments was low with an average of about 1–1.5 m $s^{-1}$ and a standard deviation of about ±0.6 m $s^{-1}$. For the second flight, the same was true for wind direction, but greater differences occurred for wind speed. While the multicopter and SODAR recorded a mean speed of 2.6 m $s^{-1}$ and 2.5 m $s^{-1}$, respectively, LIDAR and EC station had 1.7 m $s^{-1}$ and 1.4 m $s^{-1}$, respectively. At this point it has to be highlighted that the instruments were not located at the same place (distance 100–570 m from multicopter, see Fig. 1) and that time resolution varied. Besides, during north-easterly winds generation of turbulence is likely at the edge of the forest, which is to the east of the investigation area. Accordingly, differences were explainable, especially at heights up to 50 m.

### 3.2 Methane and meteorological conditions

In the night between 21 and 22 July 2015, methane measurements were made with the multicopter starting about 15 minutes after sunset (19:05 UTC) and extending over seven hours (Fig. 7). For comparison of tower and multicopter results, the subsequent measurements are displayed with orange points for tower data in 10 m and multicopter data with green ones also for 10 m. Short-term variations in methane concentration were detected by both techniques, even with the same extent (around 22:00 UTC). There was only one major deviation shortly past midnight when the multicopter measured a value of 2.45 ppm compared to 2.2 ppm at the tower. This may be due to the distance of approx. 5 m between tower and UAV and a time difference of around 30 s between those measurements. Overall, the two data sets were significantly correlated with a spearman correlation coefficient of 0.96. Calculation of the RMSE led to ±0.063 ppm. Consequently, the measurements on the moving platform were as representative as those of the stationary tower installation.

Considering the vertical methane profiles up to 50 m a.g.l., gradients were detectable during stable atmospheric conditions after sunset (Fig. 8). Data are shown for six flights with one-hour intervals beginning at 19:32 UTC and ending at 00:32 UTC. According to the potential temperature profiles, a stable stratification of the atmosphere developed after sunset indicated by increasing potential temperature with height. Its difference reached 5–6 K between ground and 50 m. Thus, this overall stable stratification led to the reduced vertical mixing, and methane sources in the surroundings caused a concentration rise of 0.3 ppm after sunset within six hours. The mean background concentration measured during this campaign was 1.9 ppm. The concentration increased at each height with time, while accumulation started from the ground. Vertical gradients were already visible right after sunset, were intensifying until the measurement at 22:32 UTC, weakening afterwards and then intensifying again at 00:32 UTC. This variability in varying gradients was in agreement with changing meteorological conditions. Mean concentrations averaged over all measurements at each level were 2.091 ppm (10 m), 2.049 ppm (25 m), and 1.976 ppm (50 m).

According to the continuous measurements at the tower, the $CH_4$ concentration increased close to the ground even before sunset. The strongest increase was seen at all heights between 21:32 and 22.32 UTC with 0.25 ppm at 10 m, 0.15 ppm at 25 m, and 0.06 ppm at 50 m. Afterwards (23:32 UTC), concentration decreased in 10 and 25 m and increased in 50 m, leading to almost the same concentration in all heights (approx. 2.07 ppm).

Variations in agreement with a stabilization of the NBL were observed from the vertical potential temperature profiles. The stability of the atmosphere increased especially between 25 and 50 m until 22:32 UTC, while $CH_4$ accumulated in the NBL. Below 25 m, the atmosphere was slightly stable to neutral. In the following hour, a destabilization in the lowest 50 m of the atmosphere was detected and afterwards stable conditions developed again. This destabilization occurred simultaneously to the mixing of methane at all heights followed by a reestablished methane gradient. The results indicated a developing surface layer up to 25 m a.g.l. where methane accumulated, but exchange with air above was not completely inhibited likely due to the fact that turbulence was not totally suppressed.

Wind in this night was mostly from west to north-west with low speed between 1–2 m $s^{-1}$ and up to 3 m $s^{-1}$ in 50 m (Fig. 9) and is shown for the same times as in Fig. 8. During the first two hours, wind direction was roughly the same with height showing a variability of about 50° (W to NW), while wind speed was about 2–3 m $s^{-1}$. Afterwards, wind speed was lower at 10 and 25 m. Mean wind direction stayed between west and north-west in 25 and 50 m, while in 10 m it changed from south (21:32 UTC) to west (22:32 UTC) and back to south and south-west (23:32 UTC). So, southern directions were accompanied by a methane decrease, lower wind speeds and higher potential temperature. In contrast to that, at 22:32 UTC wind speed was higher than 1 m $s^{-1}$ and potential temperature was 4–5 K lower than the hour before and after. During the last flight, wind direction changed back to north-west with high variability of about 100° at 10 m and 25 m, which was not seen in the second height before. This higher variability occurred mostly during low wind speeds of 1–1.5 m $s^{-1}$.

## 4 Discussion

The presented results of the multicopter-based approach showed that extending measurements from towers have advantages because measurement height and location is more flexible. Methane concentration measurements at 10 m height were in good agreement with those on the tower and could be conducted at different heights. Therefore, we conclude that the technique of using a tube with a multicopter could be also applicable for other inert trace gases and related research questions. In view of the good agreement of tower and UAV-based methane concentrations, plausible methane gradients were observed during stable atmospheric conditions although the multicopter does stir air with its propellers. Palomaki et al. (2017) demonstrated in an experiment that wind speed at 30 cm above the multicopter is 0.5 m $s^{-1}$ due to spinning rotors. According to Alvarado et al. (2017) this influence is negligible at a distance of 40–45 cm above the multicopter.

Methane concentration increases close to the ground were found below a nocturnal inversion. Using a tethered balloon instead of a multicopter, Choularton et al. (1995) detected a concentration drop of 0.05 to 0.075 ppm from the inversion layer to the layer above. This is in agreement with our multicopter measurements in 10 and 25 m a.g.l. being below 0.1 ppm in the first half of the night while a stable stratification occurred.

The vertical range of measurements was limited by the payload capacity of the multicopter and the lateral extent of the measurements was restricted by electricity availability for the methane analyzer. Using a tethered balloon, Denmead et al. (2000) pointed to the problem that it was difficult to adapt to varying NBL heights with fixed installed sampling lines. This shortcoming can be overcome with the multicopter because hovering heights can be easily changed in the flight plan. A limitation of our setup was that the vertical range of 50 m is usually not enough to cover the whole NBL height. To overcome this limitation, a multicopter with a higher payload would be necessary with the ability of carrying a longer tube. Apart from that, the vertical extension of meteorological measurements to the NBL height without the tube would be benefiting for interpretation, although no methane data would be available.

In addition, no influence of the tube on the tilt angle could be detected while hovering at 10, 25 and 50 m. A negligible influence of payload was also found by Neumann and Bartholomai (2015). To each height, the multicopter had to lift more

weight, but the autopilot compensated this with the spinning speed of the propellers, which was significantly higher on the side where the tube was mounted. Therefore, it is recommended to mount the tube in the center for a better flight performance. Besides, non-gusty wind conditions are favorable to reduce the wind load on the tube.

The wind estimation carried out during hovering showed good agreement with the tower with a RMSE of 14.5° and 0.7 m $s^{-1}$ for wind direction and speed, respectively. These values were determined using a moving average of 10 s. Applying a 20 s moving average values of 12.5° and 0.6 m $s^{-1}$ are similar to those obtained by Neumann and Bartholomai (2015) for hovering. The advantage of our approach is that no wind tunnel experiments are necessary and that the experimental flights are easy to reproduce. Since the estimated errors were a result of only a 5 min flight, further experiments and comparisons would be necessary to confirm these values. Our experimentally determined relationship between TAS and the tilt angle is only valid for this hexacopter configuration and up to a speed of 6 m $s^{-1}$.

Although the multicopter-based wind estimation was biased, measurements show similar results and the results of the other instruments showed differences too. Wind speed differed up to about 1 m $s^{-1}$ and direction up to 50° above 50 m. Below this height, influences of topography, land use and horizontal distance as well as averaging time were more pronounced and differences larger. Horizontal distance to the multicopter was 370 m for LIDAR and 540 m for SODAR, while they had averaging times of 1 min and 10 min, respectively, compared to the 10 s moving average of the multicopter. Lothon et al. (2014), for example, found similar biased differences dependent on horizontal distance and land use during the BLLAST campaign. In addition, low wind speeds (< 1 m $s^{-1}$) lead to higher variability in wind direction as seen for LIDAR data.

This is because then the wind is not well coupled to the meso-scale flow, which is often leading to variable wind directions (Anfossi et al., 2005, Mahrt, 2010). The same is true for multicopter-based wind direction at 10 m during the nighttime flights, which mainly occurred during wind speeds of less than 2 m $s^{-1}$. With regard to wind estimation from horizontal flights, this is especially important because flying with a specific speed requires a certain tilt angle. If this angle is significantly larger than the wind induced angle, determination of wind contribution to the angle could be more difficult depending on the accuracy of measuring the angle.

Hovering close to the ground led to limitations in the estimation of wind from the flight control sensors. The propeller's downwash caused motion of air beneath the multicopter. These were compensated by changing the tilt angle, but did not reflect actual wind conditions below a height of 5–6 m a.g.l. The effect was stronger during calm conditions because the jet of perturbed air did not advect away effectively. For the same reason, the data collected during descent were not used to estimate wind conditions because the multicopter moved through its own downwash.

Since the thermocouple was placed below a rotor, discontinuities were found while hovering; the temperature measurement is rather representative for the volume around the multicopter than for a point. But this ensured a continuous flow around the sensor, which increased its response time. For analysis, temperature was averaged for hovering at each level during the methane measurements.

The combination of the wind and concentration measurements suggest that the significant methane increase between 21:32 UTC and 22:32 UTC was caused by emissions from the dairy farms (about 150–200 dairy cows) to the west of the

measurement location (about 600 m distance). Actually, the methane mixing ratio started to increase around 22:00 UTC (Fig. 7), when wind direction changed from more southern to predominating western directions (250–300°) with wind speeds of around 1.5 m $s^{-1}$ (Fig. 9). Below 25 m, the atmosphere was mixed according to the vertical potential temperature profile. Taking into account these conditions, dispersion of a methane plume is low. According to Dämmgen et al. (2012), an emission rate of 14.5 g $h^{-1}$ $cow^{-1}$ can be assumed. This value was estimated for dairy cows in Bavaria (Germany) based on the IPCC guidelines (2006). Depending on the width of the methane plume(s) (100–500 m) coming from the farms, the methane concentration increase of about 0.15 ppm in half an hour would lead to emissions from about 90–450 cows. In comparison to the actual number of dairy cows measured methane concentrations were plausible. For further investigation, an approach similar to that of Hacker et al. (2016) would be suitable to calculate emission rates by flying upwind and downwind of the farms and measuring the vertical and horizontal extent of the plume.

## 5 Conclusion and outlook

This case study demonstrated the feasibility of a multicopter-based approach to detach measurements of constituent mixing ratios and meteorological variables from fixed towers to achieve mobile and flexible investigations. Especially for regions difficult to access, sensible ecosystems or locations where high towers are prohibited, multicopter-based measurements could be a suitable alternative. In addition, the results highlighted the need of both meteorological and methane measurements simultaneously. Information about potential temperature is important to determine the (in-)stability of the atmosphere and hence infer dispersion and mixing processes. Wind speed and direction provide information about the footprint, i.e. where the enhanced concentration originates. This is not only true for methane but is transferable to investigations of other trace gases and aerosols in the air. However, to apply budget methods for ground flux estimations as discussed by Denmead et al. (2000), the vertical coverage needs to be extended, for example by utilization of a lightweight onboard methane sensor.
Also for horizontal methane investigations, a lightweight and small methane sensor onboard a multicopter would be beneficial. With such a sensor it would become possible to investigate the size of the methane plumes horizontally and vertically and determine methane fluxes. Besides, the investigation of further methane sources and sinks as well as their strengths is planned in that area. To this end, horizontal wind estimation is necessary.

## Competing interests

The authors declare that they have no conflict of interest.

**Acknowledgments**

This research was supported by the TERrestrial Environmental Observatory (TERENO) pre-Alpine infrastructure funded by the Helmholtz Association and the Federal Ministry of Education and Research as well as the Ground Truth Demo and Test Facilities (ACROSS) infrastructure funded by the Helmholtz Association. The corresponding author was partly supported by a scholarship of the GRAduate School of Climate and Environment (GRACE) of the Karlsruhe Institute of Technology (KIT). Their support is highly acknowledged. We also thank the Scientific Team of the ScaleX Campaign 2015 for their contribution.

**References**

Altstädter, B., Platis, A., Wehner, B., Scholtz, A., Wildmann, N., Hermann, M., Käthner, R., Baars, H., Bange, J., and Lampert, A.: ALADINA – an unmanned research aircraft for observing vertical and horizontal distributions of ultrafine particles within the atmospheric boundary layer, Atmos. Meas. Tech., 8, 1627-1639, doi:10.5194/amt-8-1627-2015, 2015.

Alvarado, M., Gonzalez, F., Fletcher, A. and Doshi, A.: Towards the Development of a Low Cost Airborne Sensing System to Monitor Dust Particles after Blasting at Open-Pit Mine Sites, Sensors, 15, 19667-19687, doi:10.3390/s150819667, 2015.

Alvarado, M., Gonzales, F., Erskine, P., Cliff, D. and Heuff, D.: A Methodology to Monitor Airborne $PM_{10}$ Dust Particles Using a Small Unmanned Aerial Vehicle, Sensors, 17, 343, doi:10.3390/s17020343, 2017.

Andrews, A. E., Kofler, J. D., Trudeau, M. E., Williams, J. C., Neff, D. H., Masarie, K. A., Chao, D. Y., Kitzis, D. R., Novelli, P. C., Zhao, C. L., Dlugokencky, E. J., Lang, P. M., Crotwell, M. J., Fischer, M. L., Parker, M. J., Lee, J. T., Baumann, D. D., Desai, A. R., Stanier, C. O., De Wekker, S. F. J., Wolfe, D. E., Munger, J. W., and Tans, P. P.: CO2, CO, and CH4 measurements from tall towers in the NOAA Earth System Research Laboratory's Global Greenhouse Gas Reference Network: instrumentation, uncertainty analysis, and recommendations for future high-accuracy greenhouse gas monitoring efforts, Atmos. Meas. Tech., 7, 647-687, doi:10.5194/amt-7-647-2014, 2014.

Anfossi, D., Oetti, D., Degrazia, G. and Goulart A.: An analysis of sonic anemometer observations in low wind speed conditions, Bound.-Layer Meteor., 114, 179-203, doi:10.1007/s10546-004-1984-4, 2005.

Bamberger, I., Stieger, J., Buchmann, N. and Eugster, W.: Spatial variability of methane: Attributing atmospheric concentrations to emissions, Environ. Pollut., 190, 65-74, doi:10.1016/j.envpol.2014.03.028, 2014.

Banta, R. M., Pichugina, Y. L., Kelley, N. D., Hardesty, R. M., and Brewer, W. A.: Wind energy meteorology: Insight into wind properties in the turbine-rotor layer of the atmosphere from high-resolution Doppler lidar, Bull. Amer. Meteorol. Soc., 94, 883-902, doi:http://dx.doi.org/10.1175/BAMS-D-11-00057.1, 2013.

Båserud, L., Reuder, J., Jonassen, M. O., Kral, S. T., Paskyabi, M. B., and Lothon, M.: Proof of concept for turbulence measurements with the RPAS SUMO during the BLLAST campaign, Atmos. Meas. Tech., 9, 4901-4913, doi:10.5194/amt-9-4901-2016, 2016.

Berman, E. S. F., Fladeland, M. L. J., Kolyer, R., and Gupta, M.: Greenhouse gas analyzer for measurements of carbon dioxide, methane, and water vapor aboard an unmanned aerial vehicle, Sens. Actuators B Chem., 169, 128–135, doi:http://dx.doi.org/10.1016/j.snb.2012.04.036, 2012.

Beswick, K. M., Simpson, T. W., Fowler, D., Choularton, T. W., Gallagher, M. W., Hargreaves, K. J., Sutton, M. A. and Kaye, A.: Methane emissions on large scales, Atmos. Environ., 32(19), 3283-3291, doi:10.1016/S1352-2310(98)00080-6, 1998.

Chang, C.-C., Wang, J.-L., Chang, C.-Y., Liang, M.-C.: Development of a multicopter-carried whole air sampling apparatus and its applications in environmental studies, Chemosphere, 144, 484-492, doi:10.1016/j.chemosphere.2015.08.028, 2016.

Choularton, T. W., Gallagher, M. W., Bower, K. N., Fowler, D., Zahniser, M., and Kaye, A.: Trace Gas Flux Measurements at the Landscape Scale Using Boundary-Layer Budgets, Phil. Trans. Roy. Soc. A., 351, 357-369, 1995.

Dämmgen, U., Rösemann, C., Haenel, H.-D. and Hutchings, N. J.: Enteric methane emissions from German dairy cows, Landbauforsch Appl Agric Forestry Res, 1/2(62), 21-32, 2012.

de Boer, G., Palo, S., Argrow, B., LoDolce, G., Mack, J., Gao, R.-S., Telg, H., Trussel, C., Fromm, J., Long, C. N., Bland, G., Maslanik, J., Schmid, B., and Hock, T.: The Pilatus unmanned aircraft system for lower atmospheric research, Atmos. Meas. Tech., 9, 1845-1857, doi:10.5194/amt-9-1845-2016, 2016.

Denmead, O. T., Leuning, R., Griffith, D. W. T., Jamie, I. M., Esler, M. B., Harper, L. A., and Freney, J. R.: Verifying inventory predictions of animal methane emissions with meteorological measurements, Bound.-Layer Meteor., 69, 187-209, doi:10.1023/A:1002604505377, 2000.

Dlugokencky, E. J., Nisbet, E. G., Fisher, R. and Lowry, D.: Global atmospheric methane: budget, changes and dangers, Phil. Trans. R. Soc. A., 369, 2058-2072, doi:10.1098/rsta.2010.0341, 2011.

Egger, J., Bajrachaya, S., Heinrich, R., Kolb, P., Lämmlein, S., Mech, M., Reuder, J., Schäper, W., Shakya, P., Schween, J., and Wendt, H.: Diurnal winds in the Himalayan Kali Gandaki valley. Part III: Remotely piloted aircraft soundings, Mon. Weather Rev, 130(8), 2042-2058, 2002.

Emeis, S., Schäfer, K. and Münkel, C.: Observation of the structure of the urban boundary layer with different ceilometers and validation by RASS data, Meteorol. Z., 18(2), 149-154, doi:10.1127/0941-2948/2009/0365, 2009.

Forster, P., Ramaswamy, V., Artaxo, P., Berntsen, T., Betts, R., Fahey, D. W., Haywood, J., Lean, J., Lowe, D. C., Myhre, G., Nganga, J., Prinn, R., Raga, G., Schulz, M., and Van Dorland, R.: Changes in Atmospheric Constituents and in Radiative Forcing. In: Climate Change 2007: The Physical Science Basis. Contribution of Working Group I to the Fourth Assessment Report of the Intergovernmental Panel on Climate Change [Solomon, S., D. Qin, M. Manning, Z. Chen, M.

Marquis, K.B. Averyt, M.Tignor and H.L. Miller (eds.)]. Cambridge University Press, Cambridge, United Kingdom and New York, NY, USA, 2007.

Haas, P. Y., Balistreri, C., Pontelandolfo, P., Triscone, G., Pekoz, H., and Pignatiello, A.: Development of an unmanned aerial vehicle UAV for air quality measurement in urban areas, In 32nd AIAA Applied Aerodynamics Conference, 2014.

Hacker, J. M., Chen, D., Bai, M., Ewenz, C., Junkermann, W., Lieff, W., McManus, B., Neininger, B., Sun, J., Coates, T., Denmead, T., Flesch, T., McGinn, S. and Hill, J.: Using airborne technology to quantify and apportion emissions of $CH_4$ and $NH_3$ from feedlots, Anim. Prod. Sci., 56(3), 190-203, 2016.

Hammann, E., Behrendt, A., Le Mounier, F., and Wulfmeyer, V.: Temperature profiling of the atmospheric boundary layer with rotational Raman lidar during the HD(CP)$^2$ Observational Prototype Experiment, Atmos. Chem. Phys., 15, 2867-2881, doi:10.5194/acp-15-2867-2015, 2015.

Holland G. J., McGeer T., and Youngren H.: Autonomous aerosondes for economical atmospheric soundings anywhere on the globe, Bull. Amer. Meteorol. Soc., 73(12), 1987-1998, 1992.

IPCC – Intergovernmental Panel on Climate Change: 2006 IPCC guidelines for national greenhouse gas inventories, Vol. 4: Agriculture, forestry and other land use, Chapter 10, http://www.ipcc-nggip.iges.or.jp/public/2006gl/pdf/4_Volume4/V4_10_Ch10_Livestock.pdf, 2006.

Khan, A., Schaefer, D., Tao, L., Miller, D.J., Sun, K., Zondlo, M.A., Harrison, W.A., Roscoe, B., Lary, D.J.: Low Power Greenhouse Gas Sensors for Unmanned Aerial Vehicles. Remote Sens., 4, 1355-1368, doi:10.3390/rs4051355, 2012.

Kirschke, S., Bousquet, P., Ciais, P., Saunois, M., Canadell, J. G., Dlugokencky, E. J., Bergamaschi, P., Bergmann, D., Blake, D. R., Bruhwiler, L., Cameron-Smith, P., Castaldi, S., Chevallier, F., Feng, L., Fraser, A., Heimann, M., Hodson, E. L., Houweling, S., Josse, B., Fraser, P. J., Krummel, P.B., Lamarque, J.F., Langenfelds, R. L., Le Quere, C., Naik, V., O'Doherty, S., Palmer, P. I., Pison, I., Plummer, D., Poulter, B., Prinn, R. G., Rigby, M., Ringeval, B., Santini, M., Schmidt, M., Shindell, D. T., Simpson, I. J., Spahni, R., Steele, L.P., Strode, S. A., Sudo, K., Szopa, S., Van Der Werf, G. R., Voulgarakis, A., Van Weele, M., Weiss, R. F., Williams, J. E., and Zeng, G.: Three decades of global methane sources and sinks, Nat. Clim. Change, 6, 813-823, doi:10.1038/NGEO1955, 2013.

Konrad T., Hill M., Rowland J., Meyer J.: A small, radio-controlled aircraft as a platform for meteorological sensors, Appl. Phys. Lab. Tech. Digest, 10, 11-19, 1970.

Korhonen, K., Giannakaki, E., Mielonen, T., Pfüller, A., Laakso, L., Vakkari, V., Baars, H., Engelmann, R., Beukes, J. P., Van Zyl, P. G., Ramandh, A., Ntsangwane, L., Josipovic, M., Tiitta, P., Fourie, G., Ngwana, I., Chiloane, K., and Komppula, M.: Atmospheric boundary layer top height in South Africa: measurements with lidar and radiosonde compared to three atmospheric models, Atmos. Chem. Phys., 14, 4263-4278, doi:10.5194/acp-14-4263-2014, 2014.

Kunstmann, H., Schneider, K., Forkel, R., and Knoche, R.: Impact analysis of climate change for an Alpine catchment using high resolution dynamic downscaling of ECHAM4 time slices, Hydrology and Earth System Sciences, 8(6), 1030-1044, doi:10.5194/hess-8-1031-2004, 2004.

Kunstmann, H., Krause, J., and Mayr, S.: Inverse distributed hydrological modelling of Alpine catchments, Hydrology and

Earth System Sciences, 10, 395-412, doi:10.5194/hess-10-395-2006, 2006.

Lothon, M., Lohou, F., Pino, D., Couvreux, F., Pardyjak, E. R., Reuder, J., Vilà-Guerau de Arellano, J., Durand, P., Hartogensis, O., Legain, D., Augustin, P., Gioli, B., Lenschow, D. H., Faloona, I., Yagüe, C., Alexander, D. C., Angevine, W. M., Bargain, E., Barrié, J., Bazile, E., Bezombes, Y., Blay-Carreras, E., van de Boer, A., Boichard, J. L., Bourdon, A., Butet, A., Campistron, B., de Coster, O., Cuxart, J., Dabas, A., Darbieu, C., Deboudt, K., Delbarre, H., Derrien, S., Flament, P., Fourmentin, M., Garai, A., Gibert, F., Graf, A., Groebner, J., Guichard, F., Jiménez, M. A., Jonassen, M., van den Kroonenberg, A., Magliulo, V., Martin, S., Martinez, D., Mastrorillo, L., Moene, A. F., Molinos, F., Moulin, E., Pietersen, H. P., Piguet, B., Pique, E., Román-Cascón, C., Rufin-Soler, C., Saïd, F., Sastre-Marugán, M., Seity, Y., Steeneveld, G. J., Toscano, P., Traullé, O., Tzanos, D., Wacker, S., Wildmann, N., and Zaldei, A.: The BLLAST field experiment: Boundary-Layer Late Afternoon and Sunset Turbulence, Atmos. Chem. Phys., 14, 10931-10960, doi:10.5194/acp-14-10931-2014, 2014.

Mahrt, L.: Surface Wind Direction Variability, J. Appl. Meteor. Climatol., 50, 144-152, doi:10.1175/2010JAMC2560.1, 2011.

Martin, S., Bange, J., and Beyrich, F.: Meteorological profiling of the lower troposphere using the research UAV "M2AV Carolo", Atmos. Meas. Tech., 4, 705-716, doi:10.5194/amt-4-705-2011, 2011.

Mathieu, N., Strachan, I. B., Leclerc, M. Y., Karipot, A. and Pattey, E.: Role of low-level jets and boundary-layer properties on the NBL budget technique, Agric. For. Meteorol., 135, 35-43, doi:10.1016/j.agrformet.2005.10.001, 2005.

Mauder, M., Cuntz, M., Drüe, C., Graf, A., Rebmann, C., Schmid, H.P., Schmidt, M., and Steinbrecher, R.: A strategy for quality and uncertainty assessment of long-term eddy-covariance measurements, Agric. Forest Meteorol., 169, 122-135, http://dx.doi.org/10.1016/j.agrformet.2012.09.006, 2013.

McGeer T., and Holland G.: Small autonomous aircraft for economical oceanographic observations on a wide scale, Oceanography, 6(3), 129-135, 1993.

Nathan, B. J., Golston, L. M., O'Brien, A. S., Ross, K., Harrison, W. A., Tao, L., Lary, D. J., Johnson, D. R., Covington, A. N., Clark, N. N., and Zondlo, M.: Near-field characterization of methane emission variability from a compressor station using a model aircraft, Environ. Sci. Technol., 49, 7896-7903, doi:10.1021/acs.est.5b00705, 2015.

Neumann, P. P. and Bartholomai, M.: Real-time wind estimation on a micro unmanned aerial vehicle using its inertial measurement unit, Sensor Actuator A, 235, 300-310, doi:10.1016/j.sna.2015.09.036, 2015.

Palomaki, R. T., Rose, N. T., van den Bossche, M., Sherman, T., J., and De Wekker, S. F. J.: Wind Estimation in the Lower Atmosphere Using Multirotor Aircraft, Atmos. Oceanic Technol., doi:10.1175/JTECH-D-16-0177.1, in press, 2017.

Rennó N. O., and Williams E. R.: Quasi-lagrangian measurements in convective boundary layer plumes and their implications for the calculation of cape. Mon. Weather Rev, 123(9): 2733-2742, 1995.

Sasakawa, M., Shimoyama, K., Machida, T., Tsuda, N., Suto, H., Arshinov, M., Davydov, D., Fofonov, A., Krasnov, O., Saeki, T., Koyama, Y., and Maksyutov, S.: Continuous measurements of methane from a tower network over Siberia, Tellus B, 62, 403-416, doi:10.1111/j.1600-0889.2010.00494.x, 2010.

Saunois, M., Jackson, R.B., Bousquet, P., Poulter, B., and Canadell, J.G.: The growing role of methane in anthropogenic climate change, Environ. Res. Lett. 11, 120207, doi:10.1088/1748-9326/11/12/120207, 2016.

Soddell, J. R., McGuffie, K., and Holland, G. J.: Intercomparison of atmospheric soundings from the aerosonde and radiosondes, J. Appl. Meteor. Climatol., 43(9), 1260-1269, 2004.

Spiess T., Bange J., Buschmann M., and Vörsmann P.: First application of the meteorological Mini-UAV "M2AV", Meteorol. Z., 16(2), 159-169, doi:10.1127/0941-2948/2007/0195, 2007.

Stieger, J., Bamberger, I., Buchmann, N. and Eugster W.: Validation of farm-scale methane emissions using nocturnal boundary layer budgets, Atmos. Chem. Phys., 15, 14055-14069, doi:10.5194/acp-15-14055-2015, 2015.

Stull, R.: An Introduction to Boundary Layer Meteorology. 9th Ed., Dordrecht, 1988.

Velasco, E., Marquez, C., Bueno, E., Bernabe, R. M., Sanchez, A., Fentanes, O., Molina, L. T.: Vertical distribution of ozone and VOCs in the low boundary layer of Mexico City, Atmos. Chem. Phys., 8 (12), 3061-3079, doi:10.5194/acp-8-3061-2008, 2008.

Villa, T. F., Gonzalez, F., Miljievic, B., Ristovski, Z. D., and Morawska, L.: An Overview of Small Unmanned Aerial Vehicles for Air Quality Measurements: Present Applications and Future Prospectives, Sensors, 16, 1072, doi:10.3390/s16071072, 2016.

Wang, J. M., Murphy, J. G., Geddes, J. A., Winsborough, C. L., Basiliko, N., and Thomas, S. C.: Methane fluxes measured by eddy covariance and static chamber techniques at a temperate forest in central Ontario, Canada, Biogeosciences, 10, 4371-4382, doi:10.5194/bg-10-4371-2013, 2013.

Wolf, B., Chwala, C., Fersch, B., Garvelmann, J., Junkermann, W., Zeeman, M., Angerer, A., Adler, B., Beck, C., Brosy, C., Brugger, P., Emeis, S., Dannenmann, M., De Roo, F., Diaz-Pines, E., Haas, E., Hagen, M., Hajnsek, I., Jacobeit, J., Jagdhuber, T., Kalthoff, N., Kiese, R., Kunstmann, H., Kosak, O., Krieg, R., Malchow, C., Mauder, M., Merz, R., Notarnicola, C., Philipp, A., Reif, W., Reineke, S., Rödiger, T., Ruehr, N., Schäfer, K., Schrön, M., Senatore, A., Shupe, H., Völksch., I., Wanninger, C., Zacharias, S. and Schmid, H. P.: The ScaleX campaign: scale-crossing land-surface and boundary layer processes in the TERENO-preAlpine observatory, Bull. Amer. Meteor. Soc., doi:10.1175/BAMS-D-00277.1, 2016, in press.

Worden, J., Kulawik, S., Frankenberg, C., Payne, V., Bowman, K., Cady-Peirara, K., Wecht, K., Lee, J.-E., and Noone, D.: Profiles of CH4, HDO, H2O, and N2O with improved lower tropospheric vertical resolution from Aura TES radiances, Atmos. Meas. Tech., 5, 397-411, doi:10.5194/amt-5-397-2012, 2012.

Zacharias, S., Bogena, H., Samaniego, L., Mauder, M., Fuß, R., Pütz, T., Frenzel, M., Schwank, M., Baessler, C., Butterbach-Bahl, K., Bens, O., Borg, E., Brauer, A., Dietrich, P., Hajnsek, I., Helle, G., Kiese, R., Kunstmann, H., Klotz, S., Munch, J. C., Papen, H., Priesack, E., Schmid, H. P., Steinbrecher, R., Rosenbaum, U., Teutsch, G., and Vereecken, H.: A Network of Terrestrial Environmental Observatories in Germany, Vadose Zo. J., 10, 955-973, doi:10.2136/vzj2010.0139., 2011.

Zeeman, M. J., Mauder, M., Steinbrecher, R., Heidbach, K., Eckart, E., and Schmid, H. P.: Reduced snow cover affects

productivity of upland temperate grasslands, Agric. Forest Meteorol., 232, 514-526, doi:http://dx.doi.org/10.1016/j.agrformet.2016.09.002, 2017.

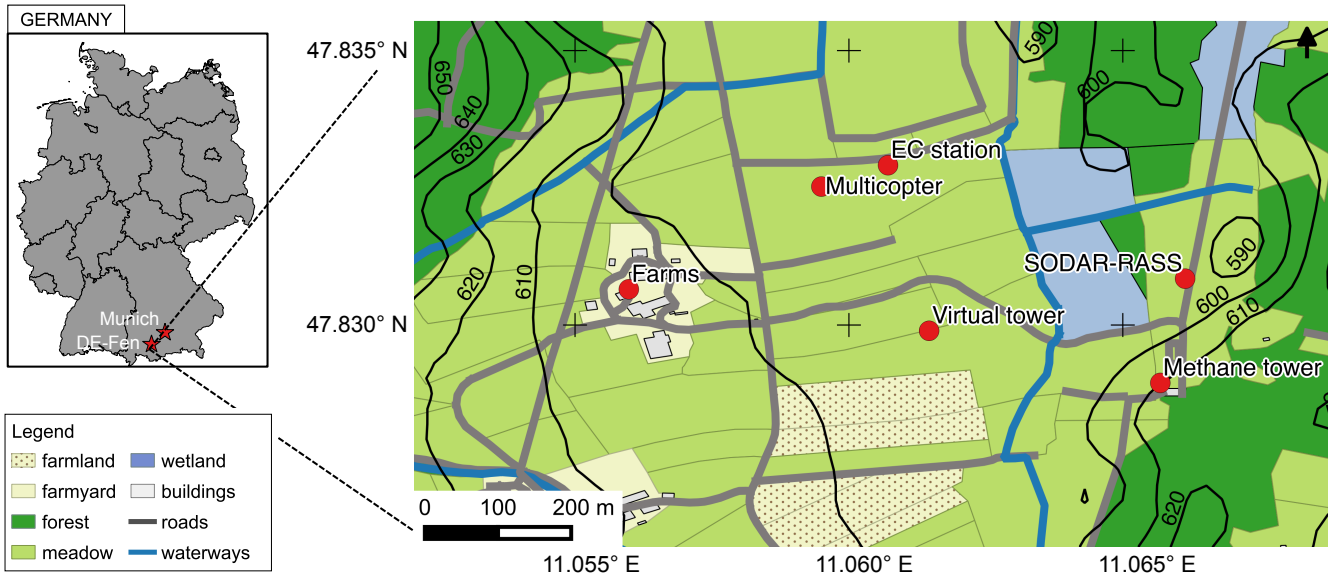


**Figure 1: Measurement site DE-Fen, Germany, with land use and ground-based instrumentation important for this study during the ScaleX campaign 2015. Contour lines stand for altitude (m) above sea level (QGIS, OpenStreetMap).**

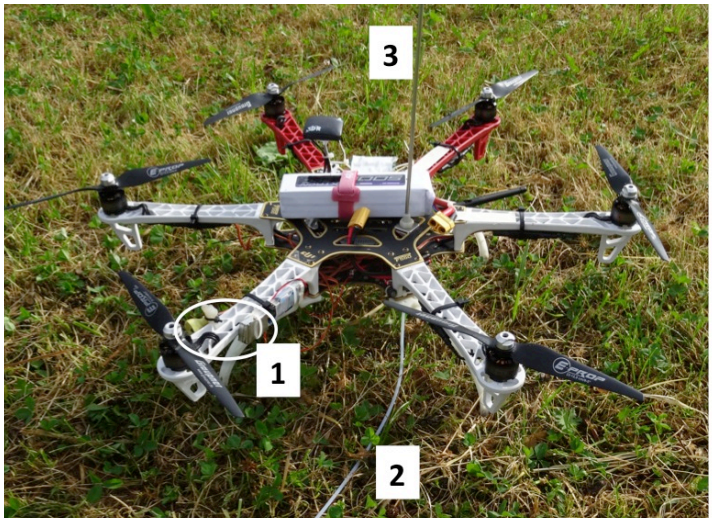


1 Air temperature and humidity sensors

2 Teflon tube

3 Tube extension above hexacopter

**Figure 2: DJI F550 multicopter with installed sensors and tube.**

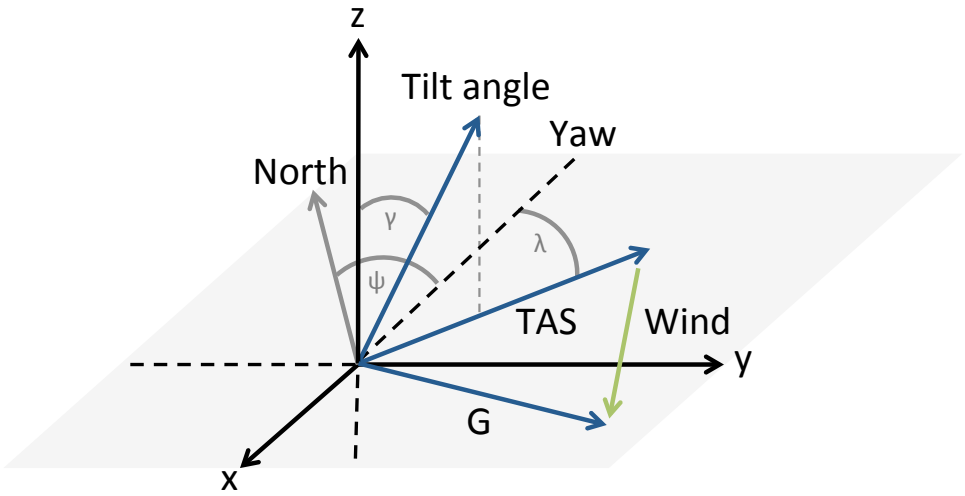


**Figure 3: Relationship between the tilt angle γ of the multicopter and the wind triangle with true air speed (TAS) vector, ground (G) vector and wind vector. Pitch angle is in x-axis and roll angle in y-axis direction. Yaw (ψ) is the viewing direction of the multicopter relative to north and the angle between TAS and yaw is λ.**

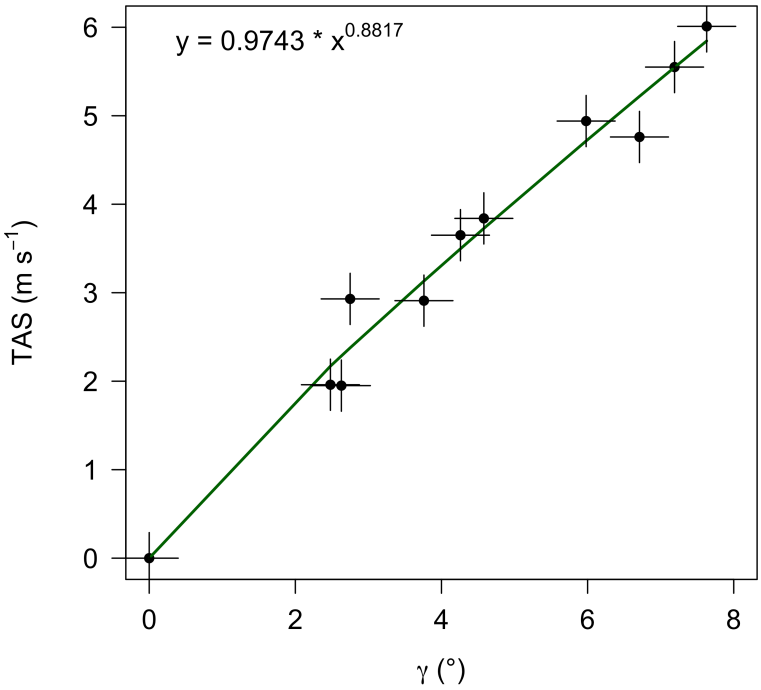


**Figure 4: Regression function of relationship between true air speed (TAS) and tilt angle ($\gamma$) experimentally determined with racetrack flights during calm wind conditions. The green line represents the fitted regression function and the error bars indicate the standard deviation of ±0.4° for the tilt angle and ±0.3 m s$^{-1}$, respectively.**

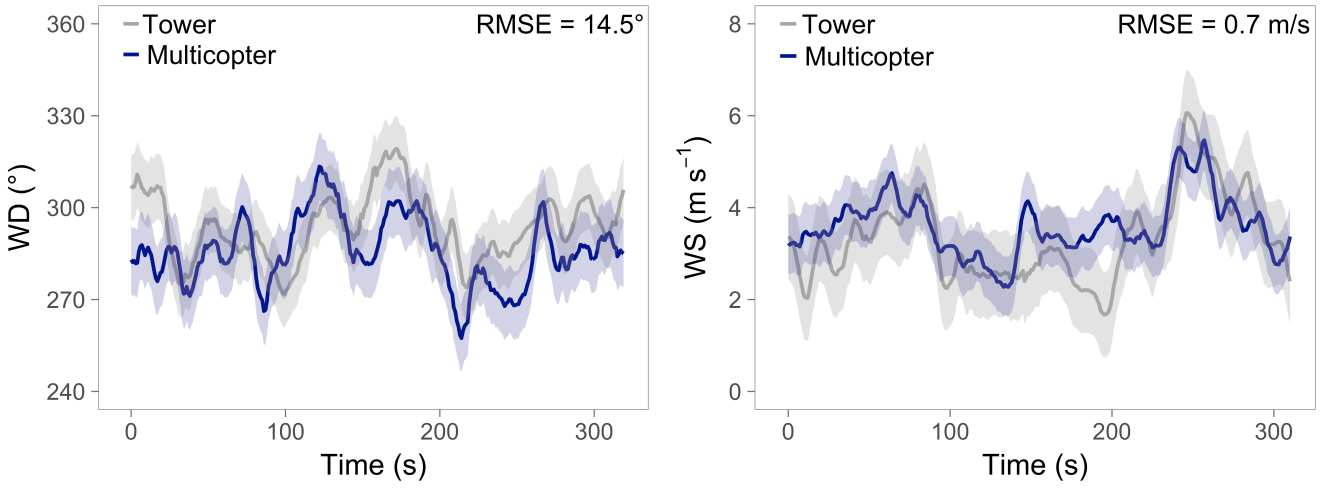


**Figure 5: Wind direction (WD) and speed (WS) comparison between tower (grey) and multicopter (blue) at 9 m a.g.l. over 5 min. The colored bands around the lines represent the standard deviation of each time series.**

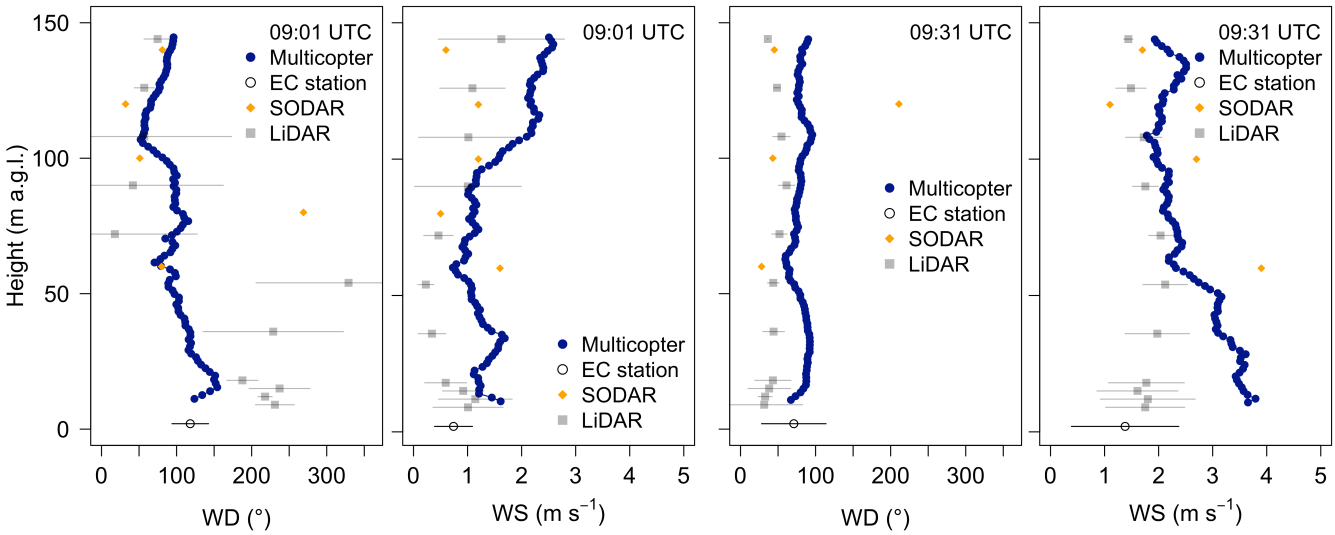


**Figure 6: Wind direction and speed profiles during two different flights: 09:01 UTC (left panels) and 09:31 UTC (right panels) on 15 July 2015. The blue profiles show multicopter data, dark grey circles represent EC station data, light grey squares LIDAR data and orange squares SODAR data. LIDAR and EC station data were averaged over the time the multicopter needed for the profile. Error bars show their standard deviation.**

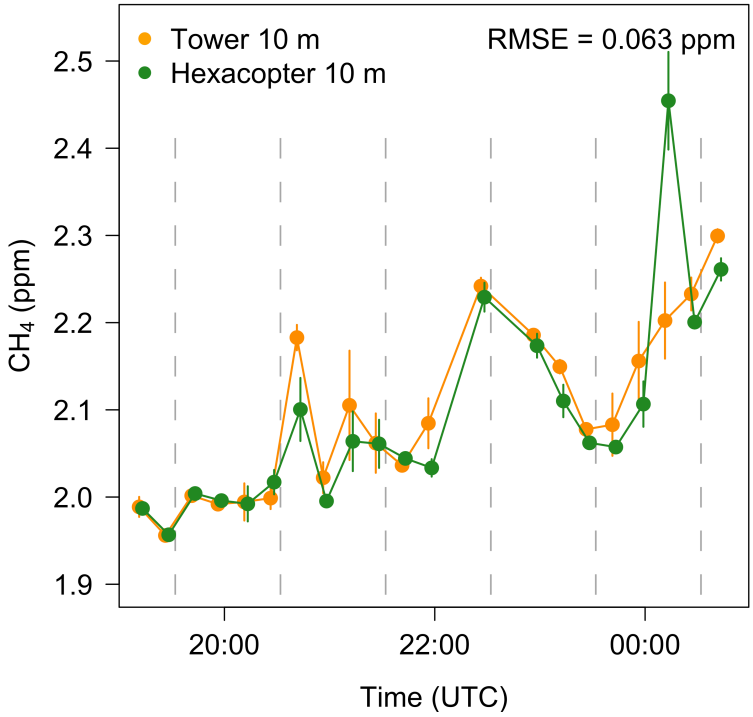


**Figure 7: Methane mixing ratio measured at the tower and with the multicopter in the night between 21 and 22 July 2015. Tower data were measured just before the 10 m data from the multicopter. Error bars show the standard deviation for each measurement averaged over 60 s. A standard deviation of 0.01 ppm or less cannot be shown because the size of the data point exceeds the error bar. The dashed grey lines represent the time for which vertical profiles are shown in Fig. 8 and 9. Local time (CEST) is UTC+2.**

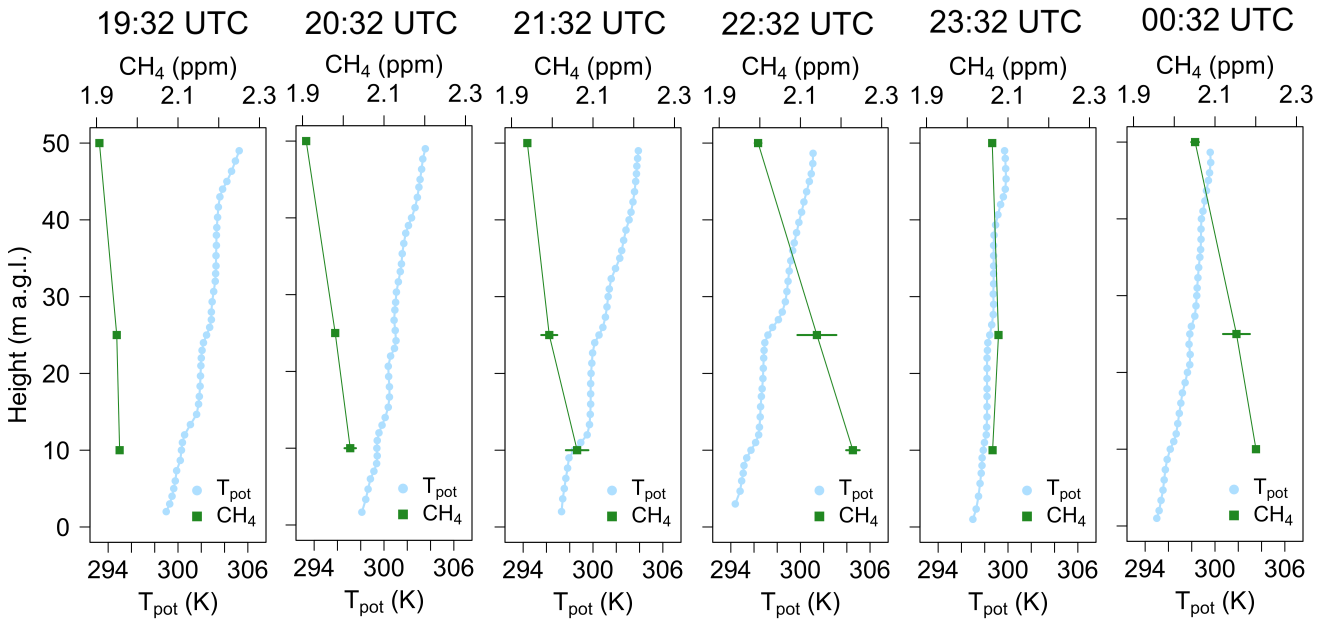


**Figure 8: Vertical potential temperature ($T_{pot}$) profiles in blue and methane concentrations in green over six hours from 19:32 UTC (left) to 00:32 UTC (right) in the night 21 to 22 July 2015. This corresponds to: 21:32 CEST to 02:32 CEST (UTC+2). Air temperature was measured with the thermocouple (ascent data only) and $T_{pot}$ was calculated with the onboard pressure data from the autopilot. $T_{pot}$ was averaged at hovering levels and smoothed with a moving average (3 s). Error bars of methane concentration show the standard deviation for each measurement averaged over 60 s. A standard deviation of 0.01 ppm or less cannot be shown because the size of the data point exceeds the error bar.**

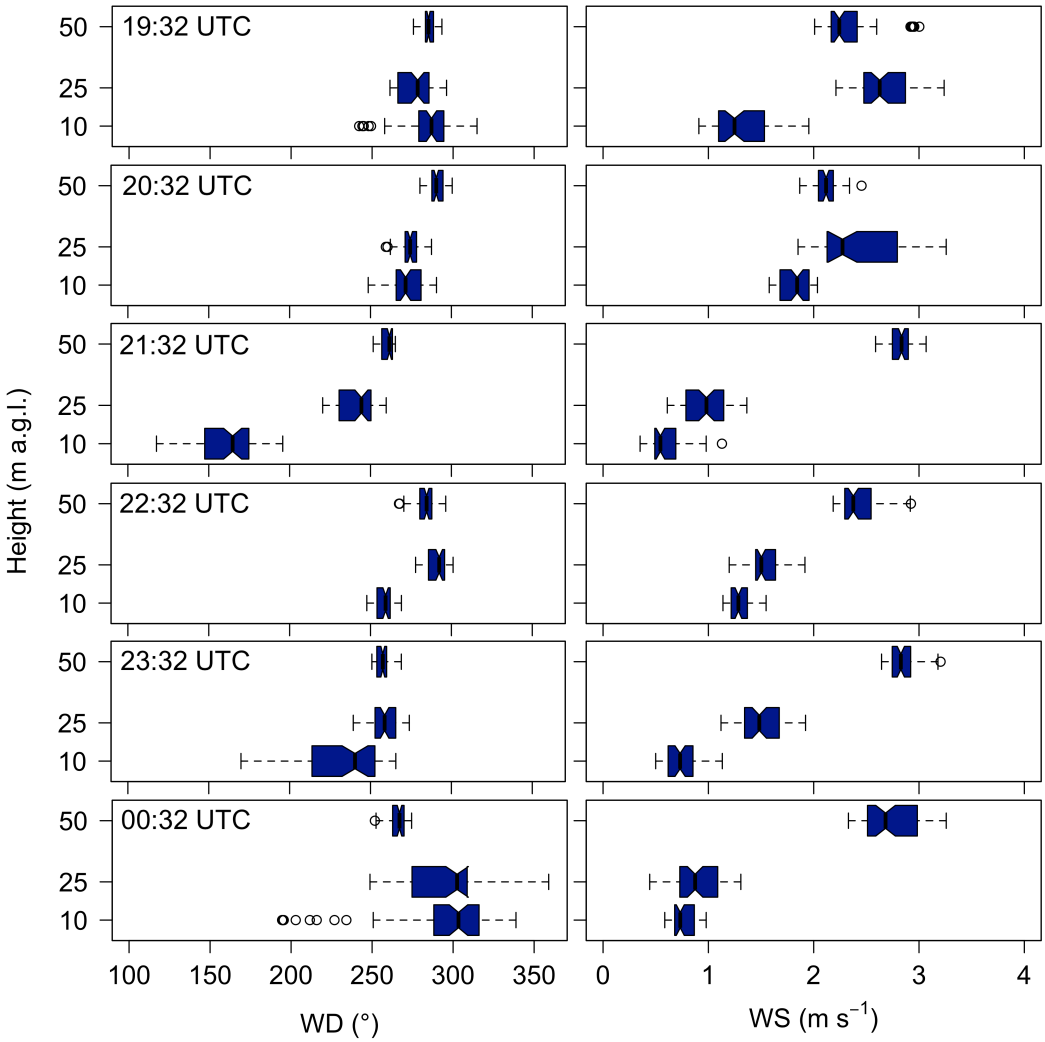


**Figure 9: Variability of wind direction (left) and speed (right) during 60 s hovering at 10, 25 and 50 m a.g.l. for flights between 19:32 UTC and 00:32 UTC in the night 21 to 22 July 2015. The blue box contains 50 % of the data and represents the interquartile range with the median as a black line. The dashed lines show maximum and minimum values in case those values are within the 1.5 interquartile range. Values outside this range (outliers) are represented with circles.**